AD NUMBER

ADB002159

LIMITATION CHANGES

TO:

Approved for public release; distribution is unlimited.

FROM:

Distribution authorized to U.S. Gov't. agencies only; Test and Evaluation; JAN 1975. Other requests shall be referred to Army Ballistic Research Laboratories, Attn: AMXBR-SS, Aberdeen Proving Ground, MD 21005.

AUTHORITY

USAARDC ltr, 8 Mar 1978

BRL R 1756

BRL

AD

REPORT NO. 1756

THE EFFECT OF MUZZLE JET ASYMMETRY ON PROJECTILE MOTION

E. M. Schmidt

January 1975

USA BALLISTIC RESEARCH LABORATORIES
ABERDEEN PROVING GROUND, MARYLAND

Destroy this report when it is no longer needed.
Do not return it to the originator.

Secondary distribution of this report by originating or sponsoring activity is prohibited.

Additional copies of this report may be obtained from the Defense Documentation Center, Cameron Station, Alexandria, Virginia 22314.

The findings in this report are not to be construed as an official Department of the Army position, unless so designated by other authorized documents.

UNCLASSIFIED

SECURITY CLASSIFICATION OF THIS PAGE (When Data Entered)

REPORT DOCUMENTATION PAGE		READ INSTRUCTIONS BEFORE COMPLETING FORM
1. REPORT NUMBER BRL Report No. 1756	2. GOVT ACCESSION NO.	3. RECIPIENT'S CATALOG NUMBER
4. TITLE (and Subtitle) THE EFFECT OF MUZZLE JET ASYMMETRY ON PROJECTILE MOTION		5. TYPE OF REPORT & PERIOD COVERED Final
		6. PERFORMING ORG. REPORT NUMBER
7. AUTHOR(s) E. M. Schmidt		8. CONTRACT OR GRANT NUMBER(s)
9. PERFORMING ORGANIZATION NAME AND ADDRESS USA Ballistic Research Laboratories Aberdeen Proving Ground, Maryland 21005		10. PROGRAM ELEMENT, PROJECT, TASK AREA & WORK UNIT NUMBERS RDT&E 1T161102A33D
11. CONTROLLING OFFICE NAME AND ADDRESS U.S. Army Materiel Command 5001 Eisenhower Avenue Alexandria, Virginia 22333		12. REPORT DATE JANUARY 1975
		13. NUMBER OF PAGES 48
14. MONITORING AGENCY NAME & ADDRESS(if different from Controlling Office)		15. SECURITY CLASS. (of this report) UNCLASSIFIED
		15a. DECLASSIFICATION/DOWNGRADING SCHEDULE

16. DISTRIBUTION STATEMENT (of this Report)

Distribution limited to US Government agencies only; Test and Evaluation; January 1975. Other requests for this document must be referred to Director, USA Ballistic Research Laboratories, ATTN: AMXBR-SS, Aberdeen Proving Ground, Maryland 21005.

17. DISTRIBUTION STATEMENT (of the abstract entered in Block 20, if different from Report)

18. SUPPLEMENTARY NOTES

19. KEY WORDS (Continue on reverse side if necessary and identify by block number)

Muzzle Blast
Transitional Ballistics
Muzzle Jet Asymmetry

20. ABSTRACT (Continue on reverse side if necessary and identify by block number) (ner)

Gasdynamic loadings experienced by a projectile passing through the muzzle gas flow field are investigated by inducing deliberate asymmetries in the muzzle flow. The effect of these asymmetries on projectile yawing motion near first maximum yaw is measured in a ballistics range. The measured data is extrapolated back to the muzzle, and the projectile angular velocity upon penetration of the muzzle blast is evaluated. The projectile linear velocity imparted by the asymmetric gasdynamic loadings is estimated using the hypersonic equiv-

DD FORM 1 JAN 73 1473 EDITION OF 1 NOV 65 IS OBSOLETE

UNCLASSIFIED

SECURITY CLASSIFICATION OF THIS PAGE (When Data Entered)

20. ABSTRACT (Continued)

alence principle. The total jump of the projectile trajectory due to both angular and linear velocity is computed and compared with measured values.

TABLE OF CONTENTS

LIST OF ILLUSTRATIONS

LIST OF ILLUSTRATIONS (Continued)

I. INTRODUCTION

Separation of a projectile from its launcher involves not only the termination of mechanical support, but also a release of the gas seal which retains the propellant gases. These highly energetic gases expand into the atmosphere forming a strong blast field. Since the initial flow velocities in this field are significantly greater than the projectile launch velocity, the projectile is rapidly engulfed in the muzzle gas flow, Figure 1. The typical blunt body shock standing at the stern of the projectile clearly illustrates that the projectile is being subject to intense gasdynamic loadings in transit of the muzzle gas flow field. As the muzzle gases continue to expand, their energy is deposited over an increasing volume of air thereby causing the blast velocity to decrease and permitting a projectile launched at supersonic velocity to escape the muzzle flow field. Since the loadings experienced by the projectile in passing through this flow directly affect its resultant trajectory, it is of interest to examine the nature of these loadings and their dependence both upon projectile design and launch conditions.

Early investigations[1-3] concentrated on schlieren or shadowgraph surveys of the muzzle gases coupled to limited probing of flow using optical measurements of the shock structure around conically tipped probes. Since these studies were conducted with small caliber rifles, the geometric scale of the flow field was overly restrictive causing the probe data to suffer from the effects of shock-boundary layer interaction; however, this early optical data clearly illustrates the basic nature of muzzle gas flow fields.

The flow is shown to consist of two readily identifiable regions, a free air blast encapsulating a supersonic, underexpanded propellant

---

1. *C. Cranz and B. Glatzel, "Die Ausstromung von Gasen Bei Hohen Anfangsdrucken," Ann. Der Physik, Vol. 43, 1914.*

2. *P. Quayle, "Spark Photography and its Application to Some Problems in Ballistics," Scientific Papers, Bureau of Standards, Vol.20, No. 508, 1925.*

3. *C. Cranz, Lehrbuch Der Ballistik, J. Springer Verlag, Berlin, 1926.*

gas jet, Figure 1 (details of this flow will be discussed in a subsequent section). Attempts[4-6] to model this flow and projectile loadings have been based upon this observed flow structure. Oswatitsch[4] performed a method of characteristics computation of a spherical blast field, Figure 2, assuming property variation across the sonic line equivalent to typical changes in muzzle exit conditions. His calculation shows that in the region between the sonic line and the inward facing shock, changes in flow properties occur at a rate significantly lower than the rate of property variation in the shock layer, i.e., the region between the inward facing shock and the blast wave. Based on this calculation, Oswatitsch proposes a 'quasi-steady' model of the propellant gas flow; namely, that the flow between the muzzle of a gun and the inward facing shock (Mach disc), Figure 3, may be calculated using steady jet or plume theory based on the instantaneous value of the muzzle exit conditions. In this manner, he models the flow as a supersonic source and estimates the loadings on the base of a ball-type projectile. Using a similar approach, Gretler[5] calculates the transverse impulses on a fin stabilized projectile, while Erdos, Del Guidice, and Visich[7] compute the forces exerted on a sabot in the muzzle gas flow. Additionally, efforts[8-9] are ongoing to apply time-dependent, finite difference techniques to the calculation of both the flow field and projectile interactions; however, both these and the steady flow attempts to model muzzle phenomena suffer from a lack of experimental data against which their predictions may be compared.

While qualitative optical data is available, quantitative measurements of the flow properties and projectile loadings are not. Some of

---

4. *K. Oswatitsch, "Intermediate Ballistics," Deutsche Luft und Raumfahrt, FB 64-37, December 1964, AD 473 249.*

5. *W. Gretler, "Intermediate Ballistics Investigations on Wing Stabilized Projectiles," Deutsche Luft und Raumfahrt, RR 67-92, December 1967.*

6. *J. I. Erdos and P. D. Del Guidice, "Gas Dynamics of Muzzle Blast," AIAA Paper 74-532, June 1974.*

7. *J. I. Erdos, P. D. Del Guidice, and M. Visich, "Aerodynamics of Sabot Discard Within a Muzzle Blast Environment," Ballistic Research Laboratories, Contractor Report 149, April 1974.*

8. *T. D. Taylor, "Calculation of Muzzle Blast Flow Fields," Picatinny Arsenal, Report 4155, December 1970, AD 881 523L.*

9. *F. H. Mallie, "Numerical Calculation of a 105mm Gun Blast with Projectile," Naval Weapons Laboratory, TR 3002, August 1973, AD 770 818.*

the reasons for this paucity of data can be taken from observations of Figure 1. The flow field is obviously complex, energetic, and highly transient. The duration of projectile residence in the muzzle gases scales with exit conditions and gun caliber. For the small arms rifle (6.5mm) considered in this report, the projectile residence time is on the order of 100 microseconds. At no time during this period is the flow field steady; projectile displacement and blast field growth continually change the nature of the flow over the projectile. In the jet alone, the projectile rapidly traverses regions of subsonic through hypersonic flow. Additionally, the forward portions of the projectile experience the highly unsteady flow in the developing blast layer. To compound the gross transience of the flow, its confining geometry and extremes of properties (e.g. across strong shock waves) make physical probing nearly impossible due to probe-flow field interference. Probing the flow about large caliber guns should be less difficult, but the probe environment becomes more extreme due to the increased period of immersion in the tube efflux. With large guns, probe heating, structural failure, and erosion due to impingement of high velocity particulate matter are all problems to be anticipated.

The use of quantitative optical techniques is difficult due both to the presence of a turbulent shear layer surrounding the jet flow field and to particulate matter obscuring much of the very early time flow. Recently, attempts[10] have been made to obtain interferometric data on the unsteady flow from the open end of a shock tube.

Finally, data taken on the projectile poses problems both in execution and interpretation. Telemetry or hardwire extraction of information on the projectile environment is both difficult and expensive. While hardwire extraction is obviously limited to low projectile launch velocities, telemetry is not. However, transducer survivability through the high pressure in-bore acceleration phase and sensitivity over the widely ranging muzzle flow field properties are difficult criteria to meet. A technique not yet mentioned is use of ballistic range measurements of projectile motion to infer impulsive loadings at the muzzle. While it is possible to take sufficient range measurements near the muzzle of a gun to evaluate the dynamic state (position, orientation, linear and angular velocity) of a projectile subsequent to penetration of the muzzle gases, it is not possible to correlate these dynamic properties to the loadings which induced them. In particular, the separation of mechanically from gasdynamically induced motions can not be achieved using typical range techniques; however, if one source of loading is held constant while the other is selectively varied, the corresponding changes in the projectile trajectory may be directly related to the varying load.

---

10. F. H. Oertel, "Laser Interferometry of Unsteady, Underexpanded Jets," Ballistic Research Laboratories, Report 1694, January 1974, AD 773664.

This report presents the results of a study to isolate gasdynamic loadings in this manner. Deliberate asymmetries are induced into the muzzle gas flow field without altering the mechanical nature of the gun tube. Data is taken in a ballistic range indicating the effect of variations in the amount and orientation of the gasdynamic asymmetry on projectile motion. The results of a 'quasi-steady' analysis of the asymmetric flow are presented and compared with data. The resulting comparison provides insight into the validity of the 'quasi-steady' approximation.

II. EXPERIMENTAL APPARATUS AND TEST PROCEDURE

To conduct the experimental program, a mounting fixture was designed to provide invariant mechanical support to the gun tube while allowing control of the symmetry of the muzzle gas flow field, Figure 4. A 254mm diameter by 12.7mm thick (non-metric dimensions: 10 in x 1/2 in) aluminum base plate is press fit onto the muzzle of a 6.71mm Mannlicher rifle. The base plate is bolted directly to the firing platform, thereby supporting the muzzle of the gun. Additional support is provided by a collar grip on the gun tube just forward of the chamber. The large diameter of the base plate was selected as a simplistic muzzle geometry for numerical computations, a bed for instrumentation in future studies, and an aid in sealing muzzle gases when the blast deflector plate is mounted.

The deflector plate provides the controlled asymmetry for these tests. The deflector is a half-circular plate with a diameter of 254mm and a thickness of 25.4mm. A hole is drilled at the origin of the plate with a diameter of 15.04mm or 2.24 projectile diameters. The deflector plate is mounted to a separate fixture and slid firmly against the base plate for firing. The deflector mount permits rotation to any desired attitude in the plane of the base plate; however, the deflector channel is always constrained to remain concentric to the gun bore. Five muzzle configurations are tested: base plate only, deflector horizontal (as shown), and deflector rotated clockwise (viewed from breech) through 90, 180, and 270 degrees relative to the horizontal.

The projectile fired in these tests is a 6.71mm, boattail, match Norma. Physical and aerodynamic properties[11] of the projectile are summarized below:

$$D = 6.71\text{mm}$$

$$L = 32.41\text{mm}$$

---

11. *W. F. Braun, "Aerodynamic Data for Small Arms Projectiles," Ballistic Research Laboratories, Report 1630, January 1973, AD 909757L.*

m = 9.01 gram

V_m = 671 m/s (2.11 grams IMR propellant)

I_a = 0.421 g-cm^2

I_t = 5.439 g-cm^2

C_{L_α} = 2.44

C_{M_α} = 3.70

This projectile was selected since it possesses a long cylindrical section which simplifies range measurements, and its length and moderate stability factor make it responsive to muzzle loadings.

Tests were conducted in the BRL Aeroballistics Range[12] using the instrumentation shown in Figure 5. Data is taken from six range stations near first maximum yaw (8 feet from the muzzle) and an impact card downrange. Each range station takes a set of orthogonal, spark shadowgraphs of the projectile and records the time of spark breakdown. Thus, a set of stations may be used to measure projectile position, orientation, and direction of motion as a function of time. In normal usage, the measured yawing motion of a spin-stabilized projectile (recorded in the α, β plane, insert Figure 5) is fit by a least squares analysis to the equation of a damped epicycle and used to evaluate aerodynamic coefficients. For the present test data, only the yawing motion of the projectile in the immediate vicinity of the muzzle is of interest; thus, a simplified data reduction is performed.

Since data is taken from stations within 726 calibers of the muzzle (half life of yaw[11] for the fast arm is 4400 calibers and for the slow arm 2 x 10^6 calibers), it will be assumed that over this distance damping of the yawing motion may be neglected. Under this assumption, the measured yawing motion is fit by a least squares analysis to the equation of an undamped epicycle:

$$\xi = \beta + i\,\alpha = k_1\, e^{i(\phi_{1_o} + \phi_1' z)} + k_2\, e^{i(\phi_{2_o} + \phi_2' z)}$$

---

12. *W. F. Braun, "The Free Flight Aerodynamics Range," Ballistic Research Laboratories, Report 1048, July 1958, AD 202249.*

Calculation of the coefficients in the above equation permits a straightforward evaluation of the magnitude and orientation of the projectile yaw and yawing velocity at any point within the region of interest. In particular, the first maximum yaw and yawing velocity at the muzzle are computed. Comparison of these properties for the various muzzle configurations indicates the effect of gasdynamic loadings due to the presence of asymmetries. Additionally, projectile impacts into the yaw card 139 feet downrange will indicate the effect of these muzzle loadings on the mean projectile trajectory.

III. EXPERIMENTAL RESULTS

Data will be presented in the range coordinate system looking from the breech of the gun down range. The yaw is represented in the α, β plane with positive sense as shown in the insert of Figure 5. The measured first maximum yaw is shown in Figure 6. Two cases are shown, the bare muzzle (no deflector) and the deflector horizontal (0^o). For both cases, between 25 and 30 rounds were fired. While the spread of the measured yaws is significant, it does not obscure the obvious trends in the data. For both test configurations, the magnitudes of yaw are roughly equal; however, the orientation of first maximum yaw is seen to be quite different. Without a deflector plate, the projectile has a definite nose down attitude. This is indicative of preferential launch loadings quite possibly of a mechanical nature. The addition of the deflector plates causes the first maximum yaw orientation to swing dramatically up and to the left. This indicates that the gasdynamic loadings induced by muzzle jet asymmetry are at least of a magnitude equivalent to the preferential loadings inferred from the bare muzzle data. Additionally, it is apparent that if the gasdynamic asymmetry is rotated to bring it into phase with the inherent mechanical loadings of the system, yaw amplification should occur.

This amplification is clearly shown in a plot of the four deflector orientations, Figure 7. For simplicity, only the mean magnitudes and orientations will be plotted. The data shows that as the deflector plate is rotated in a clockwise sense (viewed from the rear) in 90^o increments, the resultant magnitude of first maximum yaw grows as gasdynamic loadings come into phase with the mechanical loadings. In fact, the data indicates that if the plates were oriented at 225^o a doubling in the magnitude of yaw should occur. Since it is the purpose of this study to investigate the nature of muzzle gasdynamic loadings, the linear and angular velocities are of most interest since they are indicative of the impulses transmitted to the projectile.

The directed rate of change of orientation of the projectile at the muzzle, $\dot{\xi}_o$, is shown in Figure 8. Since the range data is reduced in complex coordinates, this plot is not of angular velocity in a vector sense but rather of the direction and rate of growth of yaw (i.e., direction in which the projectile nose is moving and rate at which the

yaw angle is growing). The mean values of $\dot{\xi}_o$ are plotted for the five muzzle configurations. For the bare muzzle (no deflector) firings, the projectile is launched with a value of ξ_o tending to produce a generally nose-up rotation. With the deflector plate mounted horizontal (0^o), the projectile is launched with $\dot{\xi}_o$ producing a nose-down and right motion. As the deflector plate is rotated, the phase relation between the motion induced by gasdynamic asymmetry and mechanical loadings is again observed. Assuming that in all cases the mechanical loadings are identical, the difference between any of the values of $\dot{\xi}_o$ with the deflector plate and the value without the plate should yield the yawing rate and orientation due to gasdynamic asymmetry alone, Figure 9.

The differencing produces values of $\dot{\xi}_o$ due to gasdynamic loadings, $\dot{\xi}_{og}$, which are consistent with physical reasoning. Since the geometry of deflector plate is invariant relative to the muzzle geometry during rotation, it would be anticipated that the resulting asymmetric gasdynamic loadings on the projectile would be of equal magnitude and directed in the same sense relative to the deflector. Figure 9 shows the yawing behavior to reflect this observation. As the plate is rotated, the resultant directed rate of change of orientation due to gasdynamic loadings also rotates through a similar angle without a significant change in magnitude (i.e., the plot of $\dot{\xi}_{og}$ in Figure 9 is nearly a circle with 90^o angles between respective generators). Since the deflector plate does possess a plane of symmetry, it would be anticipated that the effect of gasdynamic loadings would be to produce a couple acting in this plane. The direction of this couple is demonstrated by the measured values of $\dot{\xi}_{og}$ showing that the projectile is consistently launched with a yaw velocity acting in the plane of symmetry of the deflector plate. This yaw velocity is seen to cause the nose of the projectile to pitch toward the deflector channel.

The measured values of the yawing at the muzzle may be used to calculate the aerodynamic jump of the projectile. Aerodynamic jump is defined as the average deflection of the projectile from the particle trajectory (gravity and drag determined) due to aerodynamic forces. The derivation[13] of the equation for aerodynamic jump is based on an integration of the equations of motion of a yawing projectile and results in a complicated expression in terms of initial conditions and projectile properties. However, an order of magnitude analysis of the various

---

13. *C. H. Murphy, "Free Flight Motion of Symmetric Missiles," Ballistic Research Laboratories, Report 1216, July 1963, AD 442757.*

terms shows the expression* may be simplified to the following form:

$$J_A = - \left(\frac{I_t}{mDV}\right) \frac{C_{L_\alpha}}{C_{M_\alpha}} \dot{\xi}_o$$

This expression indicates that for positive C_{M_α}, aerodynamic jump occurs in a direction 180^o opposed to the direction of $\dot{\xi}_o$. Since the aerodynamic jump is an integral over the projectile trajectory, the yaw card data taken 139 feet from the muzzle should demonstrate this effect, Figure 10.

The projectile impacts for all five muzzle configurations are plotted. The deflector groups are distributed about the bare muzzle group (center) in a manner which follows the plate orientation. With the exception of the 0^o group, all of the deflector impact centers are between 1.5 and 2.0 mils from the bare muzzle center. The 0^o group is centered somewhat closer, roughly 1.25 calibers. Again assuming that mechanical loadings are identical in all firings and that gasdynamic loadings may be added linearly to them, the above expression for aerodynamic jump may be used to evaluate the resultant deflection on target due to asymmetric muzzle gasdynamics, Figure 10. Obviously, aerodynamic jump does not account for the total trajectory jump. The remaining jump is due to the transverse linear velocity imparted to the projectile in transit of the deflector plates. The ratio of this velocity to the launch velocity is simply the difference between the center of impact and heads of the aerodynamic jump vectors. Using the 'quasi-steady' approximation and certain other assumptions regarding the nature of the flow through channel, the next section will present an attempt to compute the loadings giving rise to the transverse linear velocity.

IV. ANALYSIS

A. Muzzle Flow Field Development

Subsequent to projectile launch, the high pressure propellant gases expand freely from the muzzle. The nature of this expansion is illustrated in a study[14] of the flow from the muzzle of an M-16 rifle. The initial expansion velocity of the propellant gases is shown to be

**In this report, range coordinates, Figure 5, are used.*

14. *E. M. Schmidt and D. D. Shear, "The Flow Field About the Muzzle of an M-16 Rifle," Ballistic Research Laboratories, Report 1692, January 1974. (Also, "The Formation and Decay of Impulsive Supersonic Jets," AIAA Paper 74-331, June 1974), AD 916646L.*

considerably higher than the projectile launch velocity. This is clearly demonstrated in a plot of the motion of observable discontinuities (illustrated schematically in Figure 3) along the axis of symmetry, Figure 11. The contact surface separates the propellant gases from the gases which were external to the gun tube at launch. Thus, it is observed that the M-16 projectile (3.36 calibers long) is immersed in propellant gases from a period prior to launch (due to leakage around the boattail) until the base crosses the contact surface at 90 microseconds subsequent to launch. It is not until 120 microseconds that the projectile penetrates the free air blast and enters flight free of muzzle disturbances.

The development of the propellant gas jet during the period of projectile residence is best illustrated by examining the jet shock structure, Figure 12. The plot shows the lateral or intercepting shocks remain in a fixed geometry once established by the downrange growth of the Mach disc. This indicates that while interactions with the free air blast are strong in the downrange direction, they are quite weak along the lateral jet boundaries. Thus, this data supports the analysis of Oswatitsch[4] which shows that relative to the flow in the forward shock layer, the flow between the muzzle and the bounding shocks may be treated as quasi-steady. The temporal variations that do occur are associated with changes in muzzle properties, Figure 13. Since these variations occur at a gradual rate over the period of projectile residence and since the signal propagation velocity through the jet is high, approximately 2800 m/s, it is assumed that the jet flow field may be computed using steady state theory and the instantaneous values of the muzzle conditions. Because the Mach number at the muzzle of both M-16 and current rifle is one over much of the period of gun tube emptying, the calculation of the muzzle jet properties is greatly simplified.

To compute the inviscid flow field of a steady, underexpanded jet, it is necessary to know the exit Mach number, ratio of specific heats, pressure ratio, and flow orientation. In the flow from gun tubes, it is assumed that for most applications the exit Mach number is one, the ratio of specific heats is a known constant value ($\gamma = 1.25$), and the flow inclination in the exit plane is zero. Thus, the single remaining parameter necessary to define the flow is the pressure ratio. Owen and Thornhill[15] make the important observation that within the bounding shock structure of an underexpanded jet, the flow field is independent of the exit pressure ratio. In other words, all signals from the jet boundary terminate at the boundary shocks and, therefore, never penetrate to the flow in the vicinity of the axis of symmetry.

---

15. *P. Owen and C. Thornhill, "The Flow in an Axially Symmetric Supersonic Jet From a Nearly Sonic Orifice into a Vacuum," Royal Armament Research and Development Establishment, Report 30/48, 1948.*

Since the projectile travels along this axis, it is not necessary to compute the full jet flow for all values of pressure ratio in order to obtain an estimate of the flow seen by the projectile. The properties along the axis of symmetry of an underexpanded jet have been calculated by N. Gerber of BRL using a method of characteristics code developed by NASA, Figure 14. The computation was performed for a pressure ratio of 500; however, other values of the pressure ratio were used with no noticeable changes in the centerline property values. This calculation will be used as a basis for the analysis of the transverse loadings experienced by the projectile.

B. Asymmetric Muzzle Flow

Spark shadowgraphs of the initial propellant gas flow from the bare muzzle are shown in Figures 15A and 15B. In the first photograph, the projectile boattail is beginning to pass the muzzle thereby releasing the propellant gases. Roughly 20 microseconds later, the flow has expanded nearly over the projectile, Figure 15B. Apparently, the flow over the projectile surface is supersonic terminated at strong oblique shocks half way up along its cylindrical section. The presence of these shocks is indicated by the opaque regions of concentrated powder particles. The muzzle flow at a considerably later time, Figure 1, shows the projectile to be fully immersed in propellant gases and experiencing a supersonic flow over its base.

The effect of mounting the deflector plate is shown in Figure 16. This photograph is taken roughly 20 microseconds after the base of the projectile passes the muzzle (8 microseconds after the photograph in Figure 15B). The presence of the deflector channel prevents the radial expansion and resultant deceleration of the propellant gases. This control of the gas expansion causes the flow in the channel to outstrip the flow in the upper half plane resulting in the obvious bulge in the blast field. For all muzzle configurations, it is apparent that the projectile is rapidly engulfed in the propellant gas flow. If the initial period of passage of the shock layer over the projectile is neglected or at least assumed to occur symmetrically, the greatest portion of the muzzle flow may be treated by a 'quasi-steady' analysis. However, since the flow field is three dimensional, it is not readily analyzed. To obtain an estimate of the order of magnitude within which 'quasi-steady' approximations are bounded, relatively gross simplifying assumptions will be made.

The basic approach will be to patch together two, known steady flows, a free jet and an annulus, Figure 17. The projectile will be assumed to traverse the flow with zero yaw, and only the lateral surface pressures will be considered in estimating the transverse loadings. Since the scale of a highly underexpanded jet is much greater than the projectile dimensions, it will be assumed that the presence of the projectile does not after the jet flow. Further, the projectile surface pressure will be assumed to recover immediately to the local jet static

pressure. For the annulus, the initial expansion from the muzzle is two dimensional; however after passing this transition section, the flow will be computed using quasi-one-dimensional theory. A similar approximation was applied successfully by Barakauskas[16] in the analysis of a confined jet flow. At the exit of the annular section, the flow will expand into an axisymmetric jet which will be computed using the method of characteristics. The composite flow resulting from the patching together of the jet and annulus along the horizontal plate surface is shown at the bottom of Figure 17.

In the initial expansion from the muzzle, the two flows should be nearly identical; however, once the annulus flow is established, a pressure discontinuity would develop along the boundary plane due to continued jet expansion, Figure 18. The relief of this pressure discontinuity is accounted for by using the 'equivalence principle'[17]. This technique obtains a solution to a two-dimensional, steady, hypersonic flow by transformation of a known solution of an analogous one-dimensional, unsteady flow. Basically, the streamwise dimension in the steady flow is divided by the streamwise velocity component to transform it into the time variable in the unsteady analog. In the present application, this principle is used to compute the expansion propagating into the annulus, Figure 19. Although compression waves also propagate into the jet, it is assumed that due to radial expansion they will get progressively weaker as they progress around the projectile.

The calculation is performed on a simplified annulus geometry. The annulus is taken to be a one-dimensional channel with a depth equal to one-quarter of the projectile circumference and static properties equal to those computed to exist in the annulus. The expansion into this channel occurs gradually at a rate determined by the transformed rate of pressure discontinuity growth, Figure 20. The conditions in the annulus and free jet are assumed to develop identically until the annular flow is established ($M=2.70$, $p/p^* = 6\times10^{-2}$). Thereafter, continued jet expansion causes the lateral discontinuity to grow quite rapidly. This spatial growth is transformed into a temporal pressure variation by the equivalence transformation ($t = X/V$).

The mean annulus pressure computed by the equivalence analysis is shown in Figure 20. While the annulus pressure also drops, the confined expansion does not lower the pressure levels to the values in the free jet. The surface pressure on the lower half of the projectile does not equalize with the upper half until the projectile passes the lip expansion. This expansion was computed using the method of characteristics and exit conditions corresponding to those existing at the annulus exit ($\gamma=1.25$, $M=3.03$). Differencing the two pressure profiles

---

16. *A. Barakauskas, "Sudden Expansion of a Bounded Jet at High Pressure Ratio," AIAA Journal, Vol. 2, No. 9, September 1964.*

17. *R. N. Cox and L. F. Crabtree, Elements of Hypersonic Aerodynamics, Academic Press, New York, 1965.*

(annulus and free jet) produces the transverse pressure pulse through the deflector, Figure 21.

The transverse force acting on the projectile as it passes through this pulse is obtained by integrating the pressures over the surface of the equivalent area projectile shown in the insert, Figure 21. Once the forcing function is obtained, it may be time integrated to derive the transverse velocity:

$$\frac{v}{V_m} = 4.03 \times 10^{-13} p^*$$

Up to this point, the only muzzle properties used were the Mach number, ratio of specific heats, and flow inclination, indicating that the analysis of a particular muzzle or projectile geometry using a quasi-steady approach has a considerable amount of flexibility. This fact is especially true of the calculation performed in suitable non-dimensional coordinates.

The mean muzzle pressure over the period of projectile transity of the pulse was measured to be

$$p^* = 4.1 \times 10^9 \ g/m^2$$

thus:

$$\frac{v}{V_m} = 1.65 \ (mils)$$

This value of transverse linear momentum jump is plotted on the previous impact card data, Figure 22. The agreement of the combined jumps, aerodynamic and linear, with the measured jump in the projectile centers of impact is remarkably good considering the coarse nature of the analysis.

V. CONCLUSIONS

An experimental program was conducted to permit the examination of the influence of gasdynamic asymmetries in the muzzle flow field upon the resultant projectile trajectory. Separation of mechanical from gasdynamic effects on the measured motion was achieved by deliberately introducing asymmetries into the muzzle flow without altering the mechanical properties of the weapon. The tests results clearly indicate that gasdynamic loadings can be generated in the muzzle blast which are of the same order of magnitude as mechanical loadings. Both the first maximum yaw and yawing velocity at the muzzle indicate that gasdynamic loadings can be used to reinforce or counteract mechanical loadings. This suggests the interesting possibility of using muzzle jet asymmetries not as a yaw inducer (as in conventional ballistic range applications) but to reduce yaw by counteracting mechanically induced

loadings and motion. Such an application would not significantly alter dispersion but could alter fixed bias and reduce first maximum yaw levels of marginally stable rounds.

An analysis of the flow through the muzzle device was developed using the quasi-steady approach of Oswatitsch. Even with gross simplifying assumptions, the method shows reasonable agreement with the measure data. This agreement indicates the applicability of this analytical technique to muzzle flows in which the significant loadings are generated after the projectile is immersed in the supersonic muzzle jet. It is not anticipated that this technique would produce accurate results in the case of a typical launch, i.e., ball projectile separating from a symmetric muzzle. In this case, the most severe loadings occur very near the muzzle (one-two calibers) during the highly unsteady blast development. This case would be better treated using a fully time dependent numerical analysis.

ACKNOWLEDGMENTS

The author wishes to thank Mr. James Bradley of BRL for his invaluable assistance in the interpretation and reduction of the range data. Additionally, the advice of Messrs Walter Braun, George Kahl, and Leonard MacAllister is greatly appreciated.

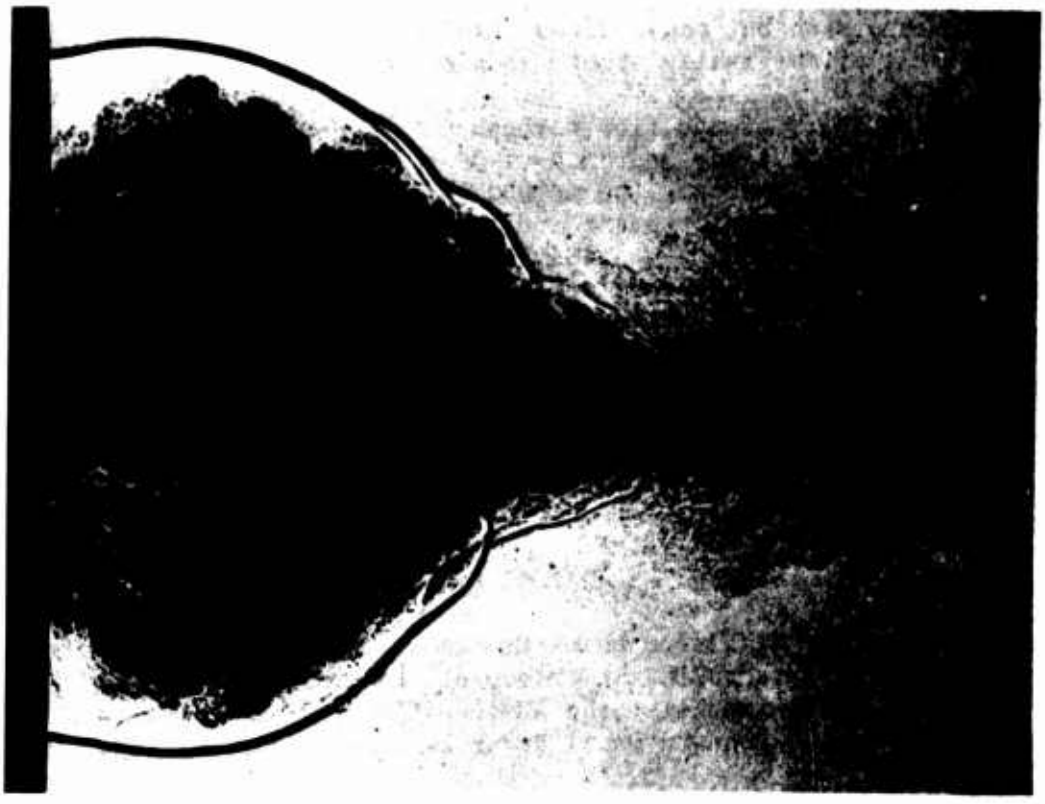

FIGURE 1: Shadowgraph of Muzzle Flow

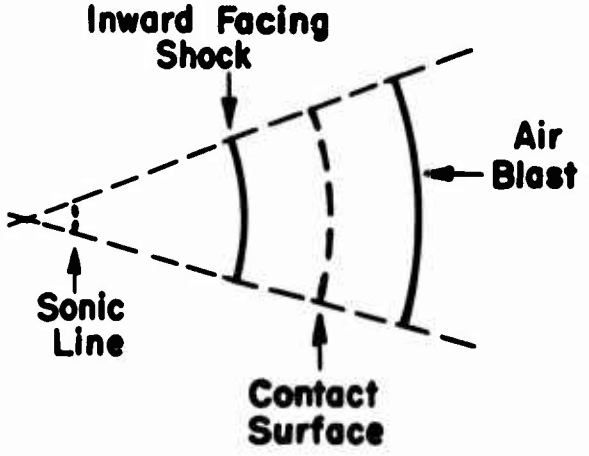

FIGURE 2: Oswatitsch Blast Computation

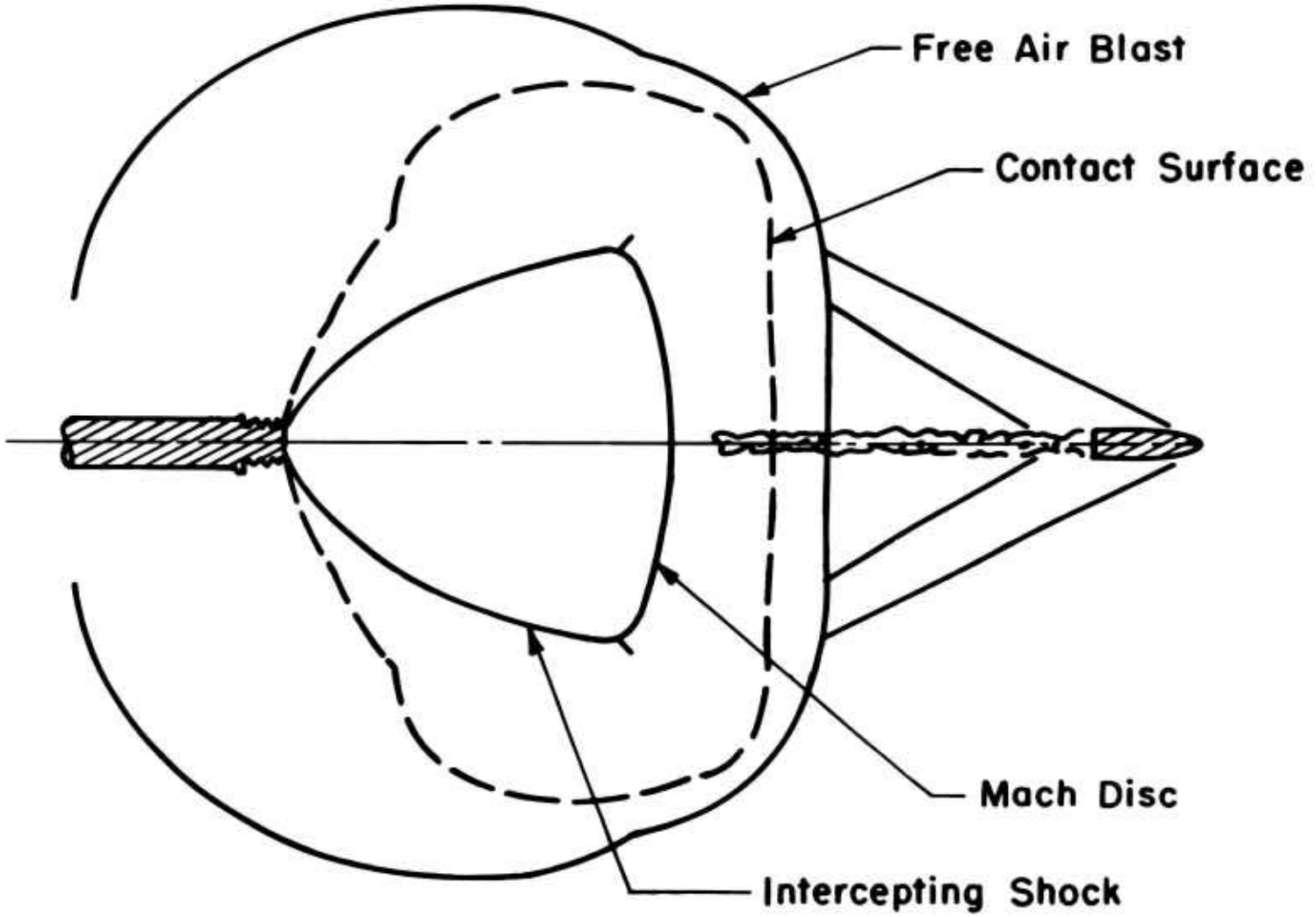

FIGURE 3: Flowfield Schematic

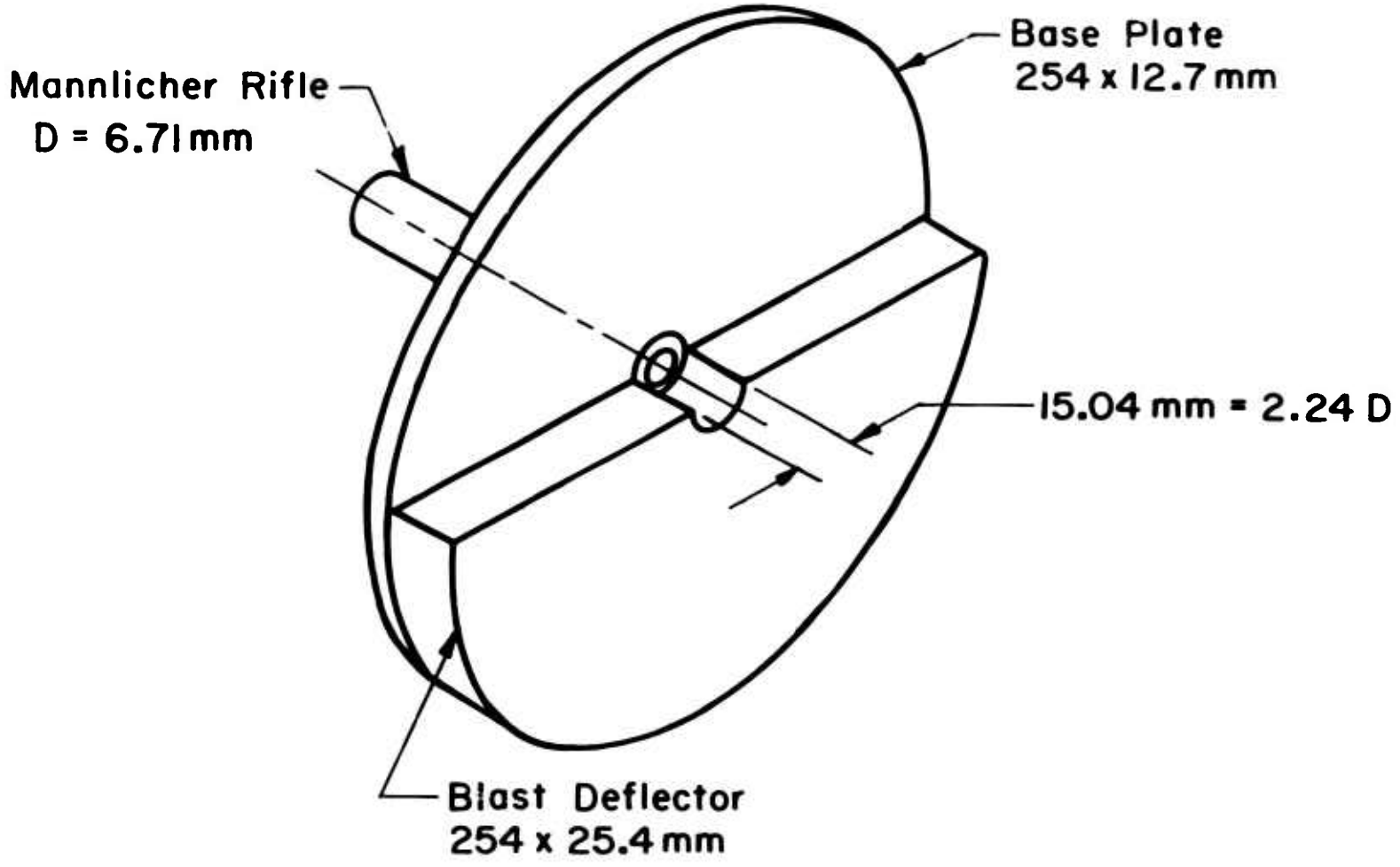

FIGURE 4: Muzzle Deflector Apparatus

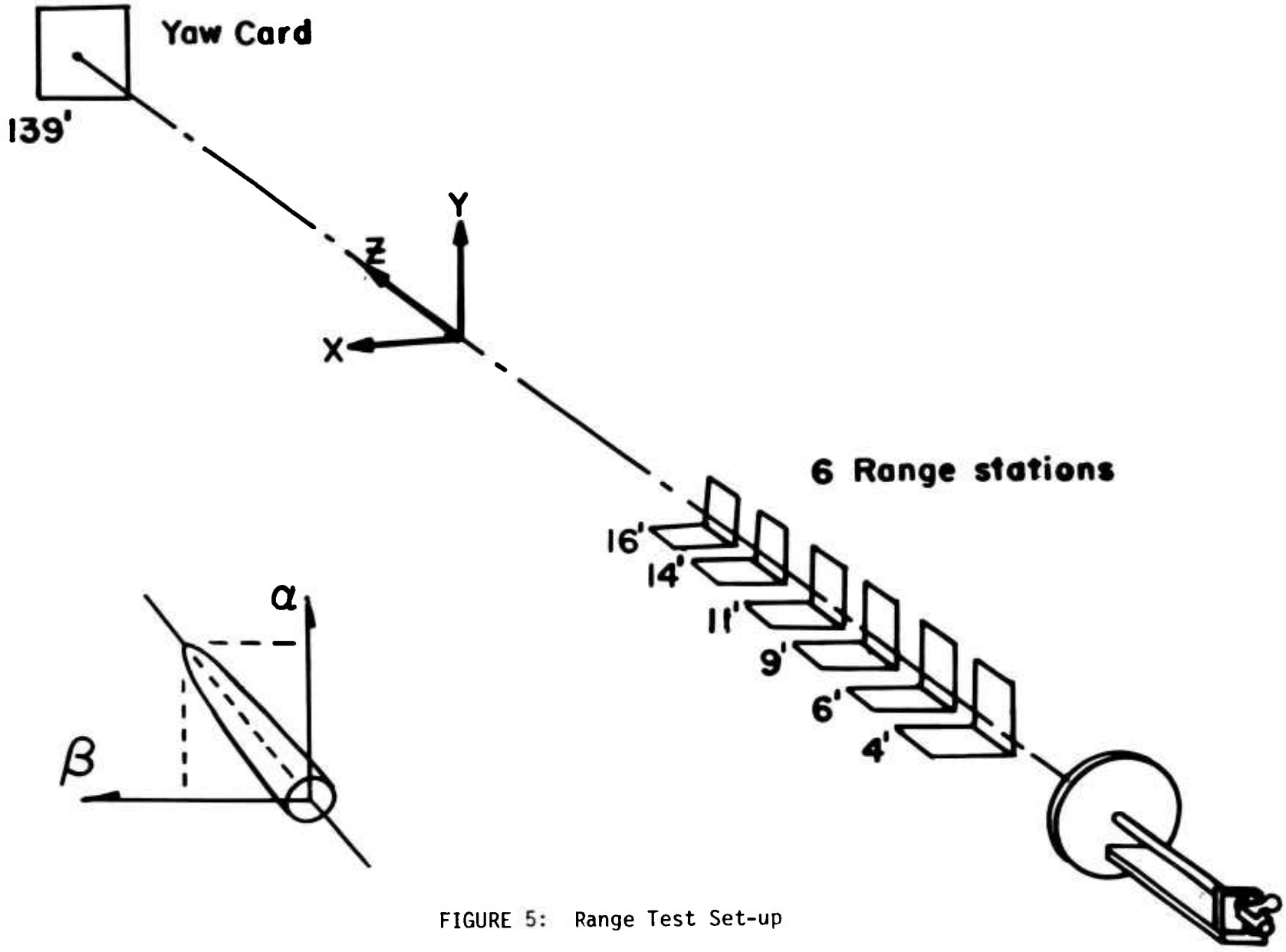

FIGURE 5: Range Test Set-up

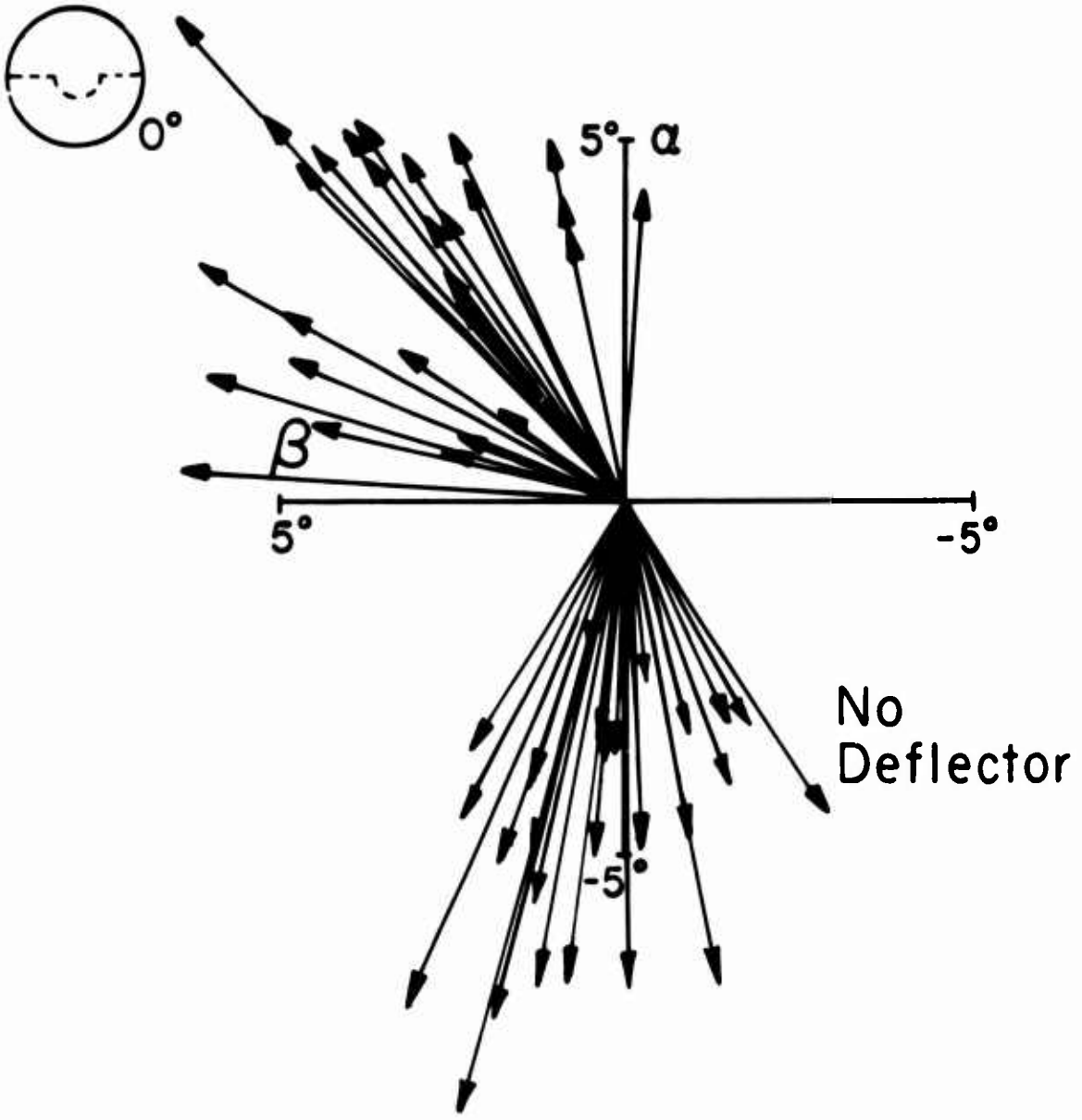

FIGURE 6: First Maximum Yaw Distribution

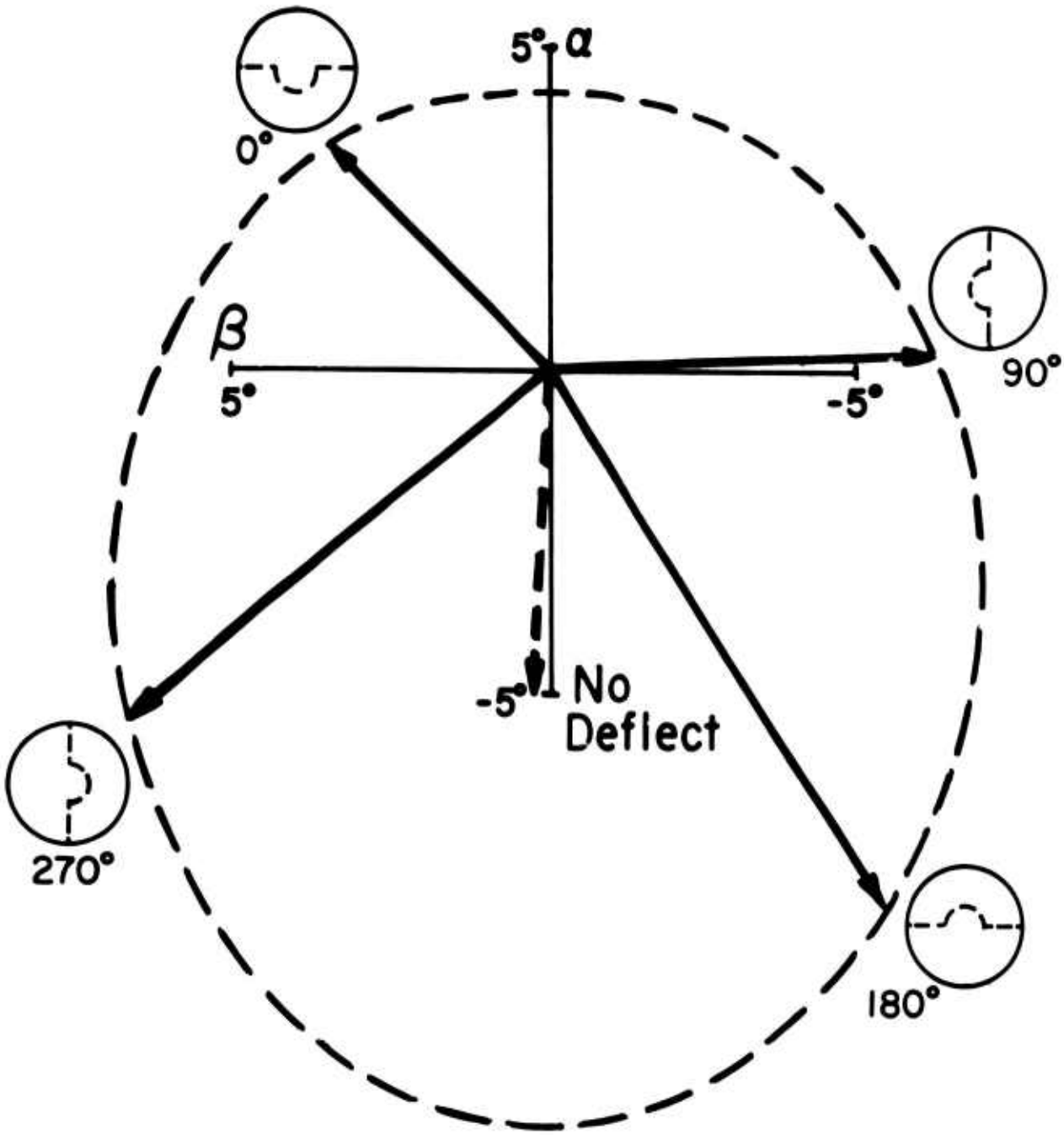

FIGURE 7: Mean First Maximum Yaw

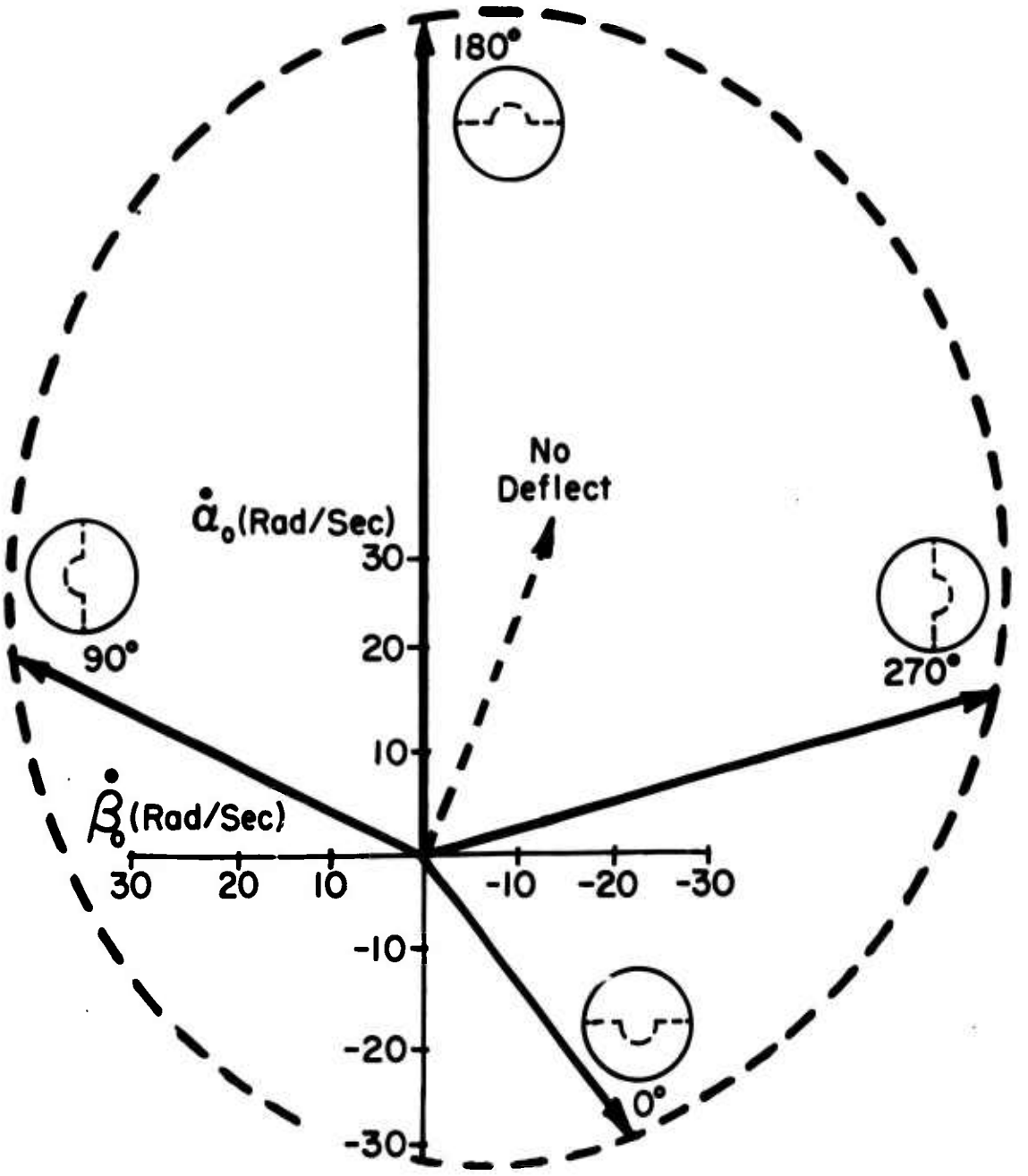

FIGURE 8: Yawing Velocity at Muzzle

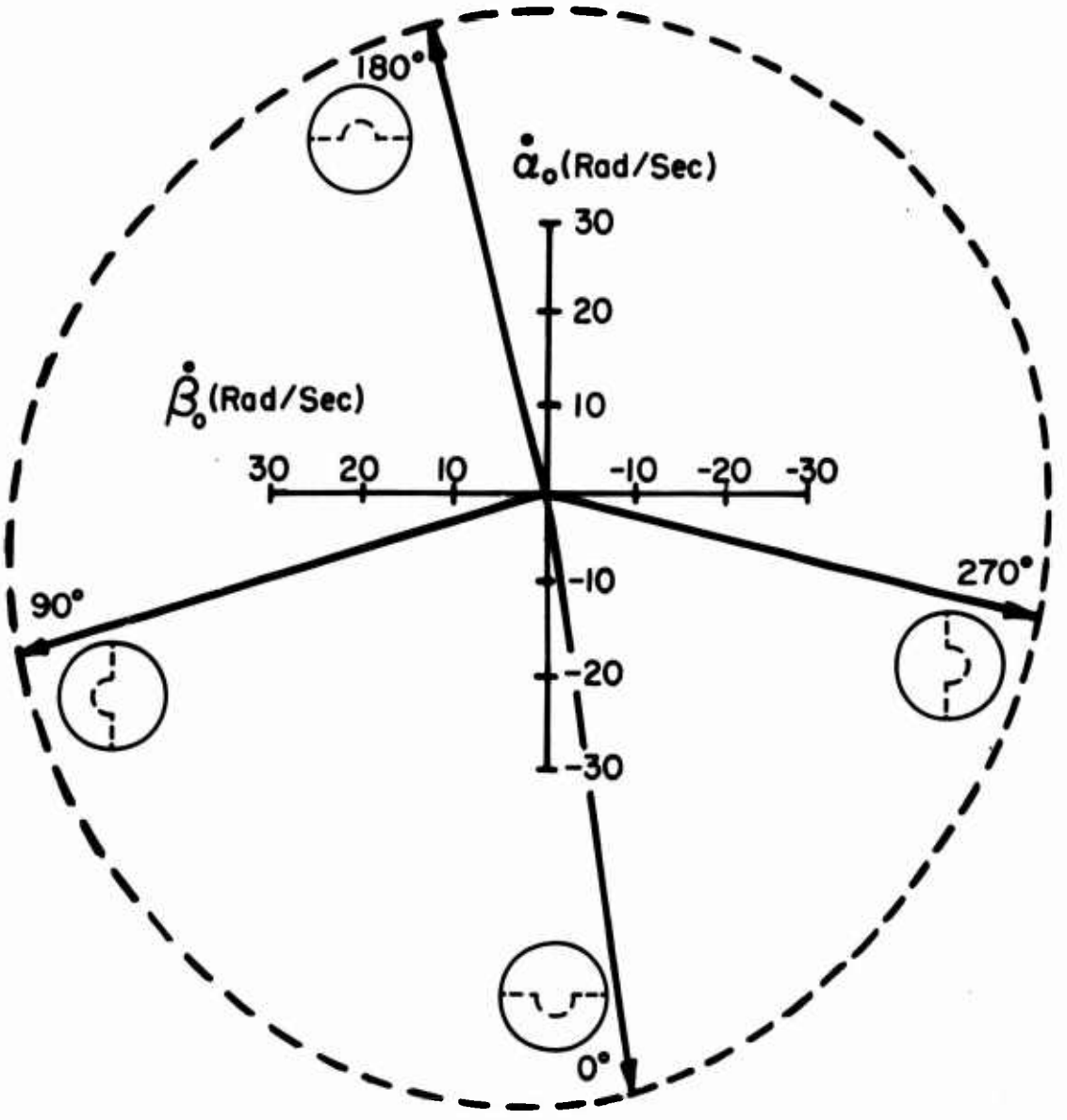

FIGURE 9: Gasdynamically Induced Yawing Velocity at Muzzle

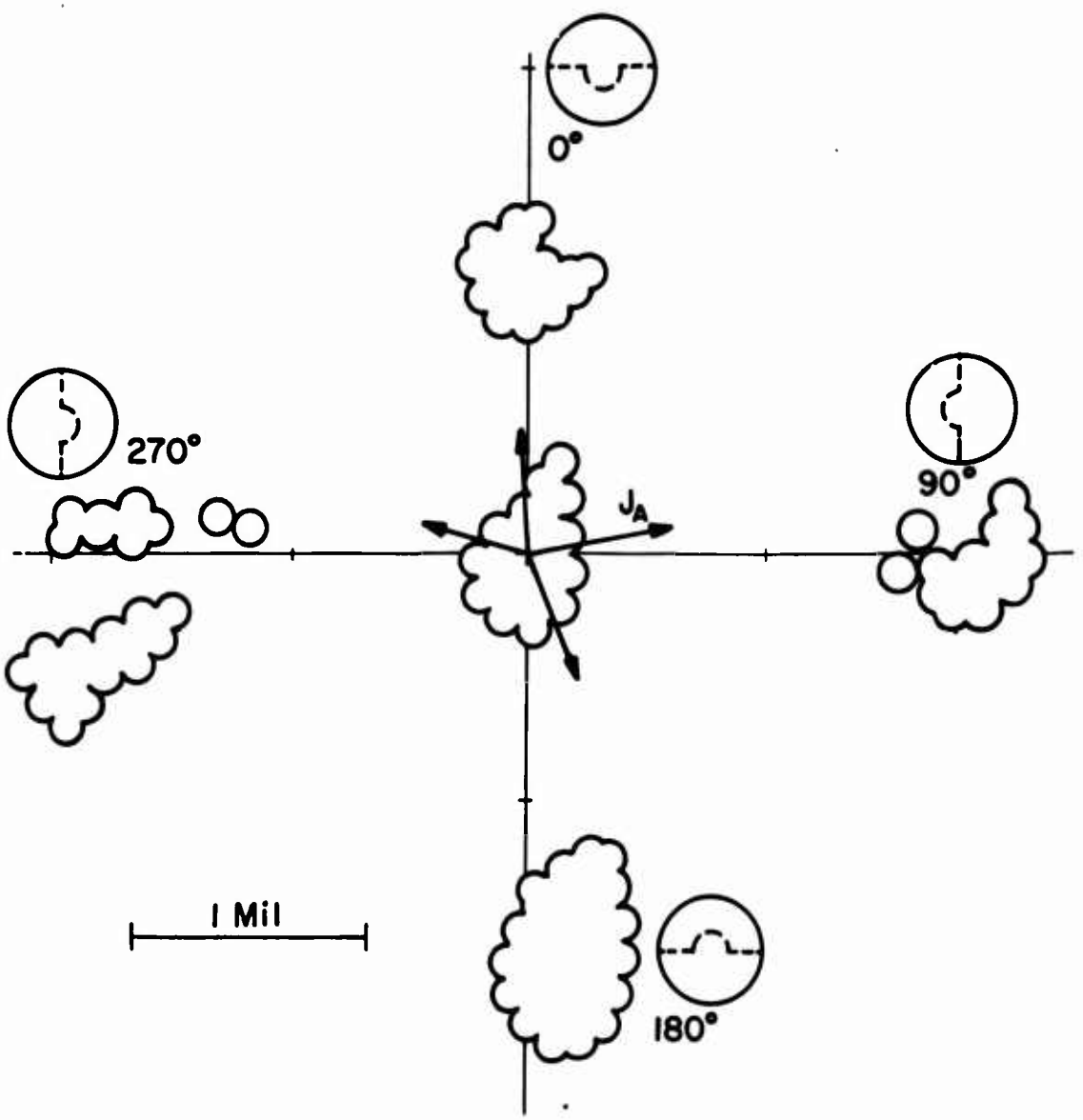

FIGURE 10: Yaw Card Impacts 139 Feet From Muzzle

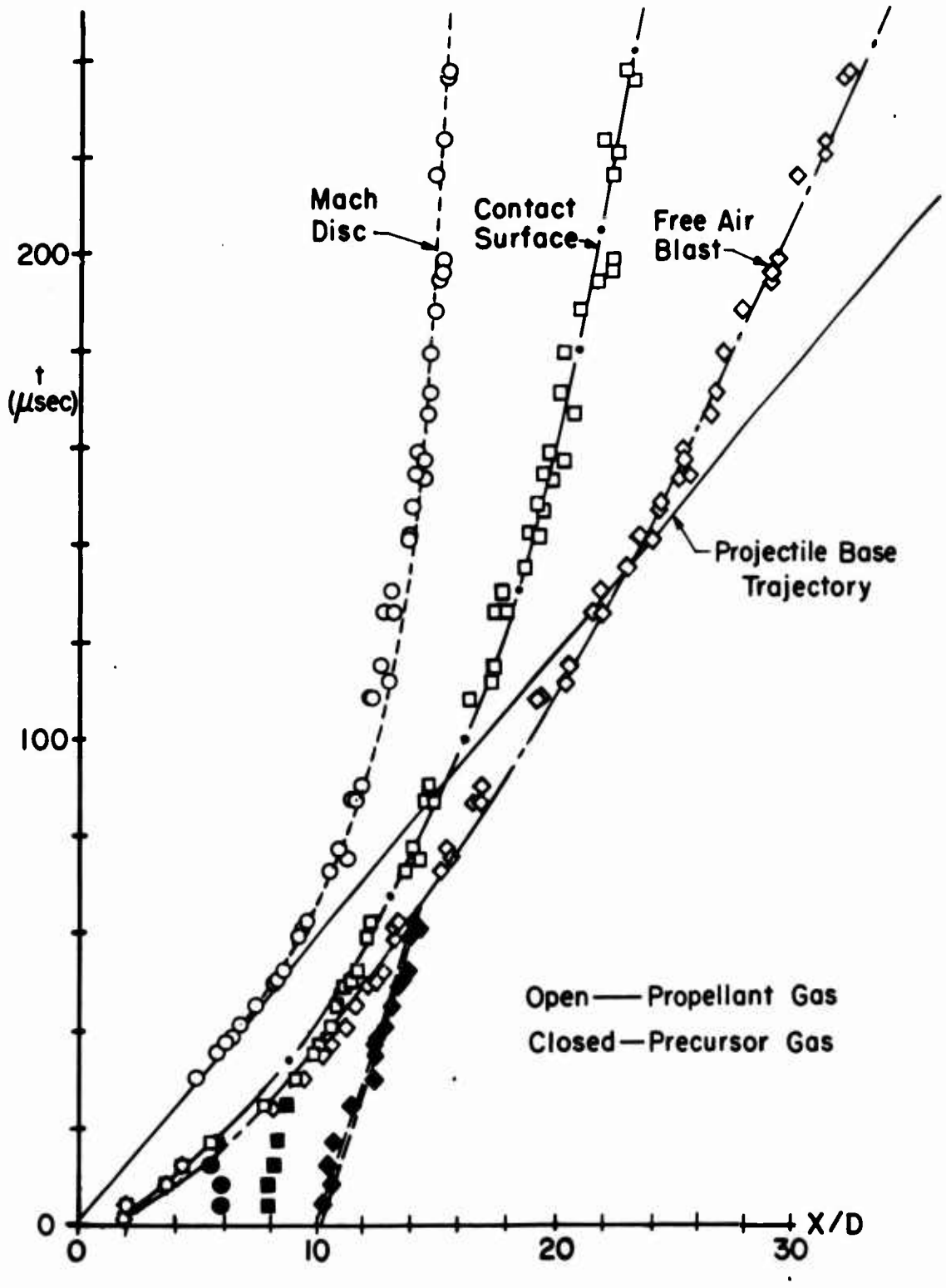

FIGURE 11: M-16 Discontinuity Trajectories Along Axis of Symmetry

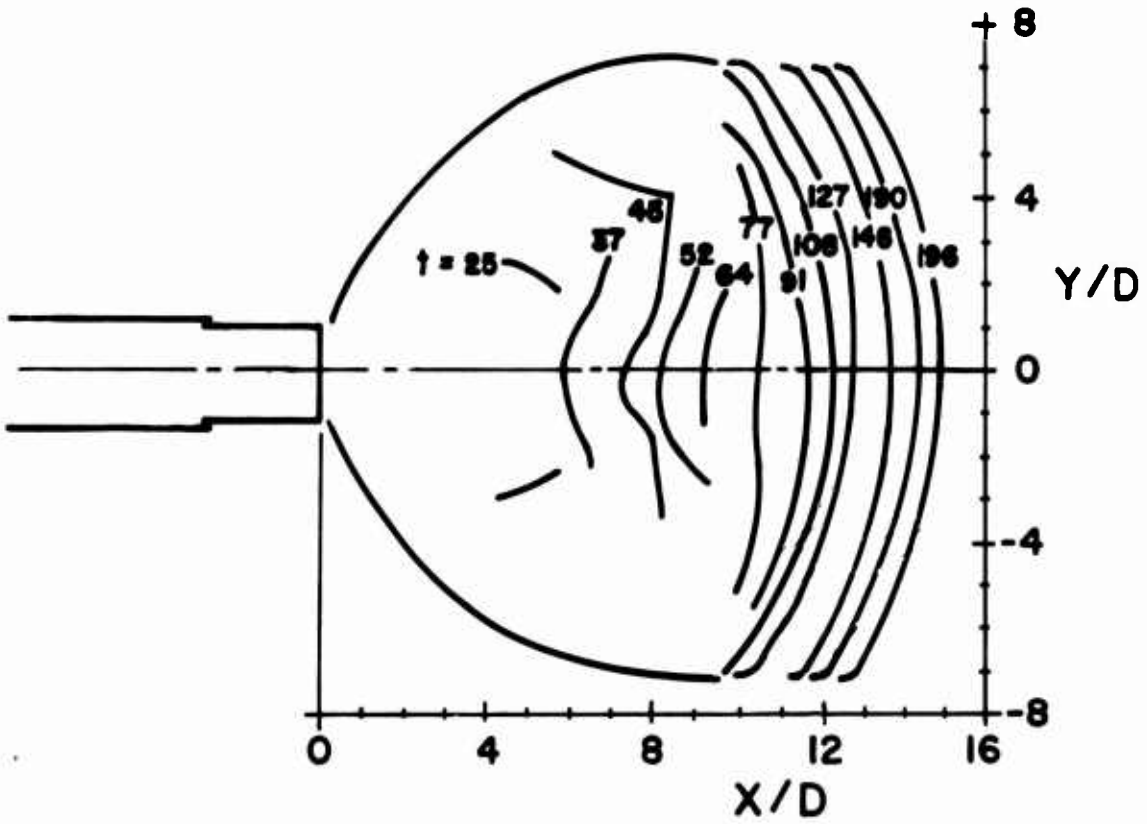

FIGURE 12: M-16 Propellant Gas Shock Structure

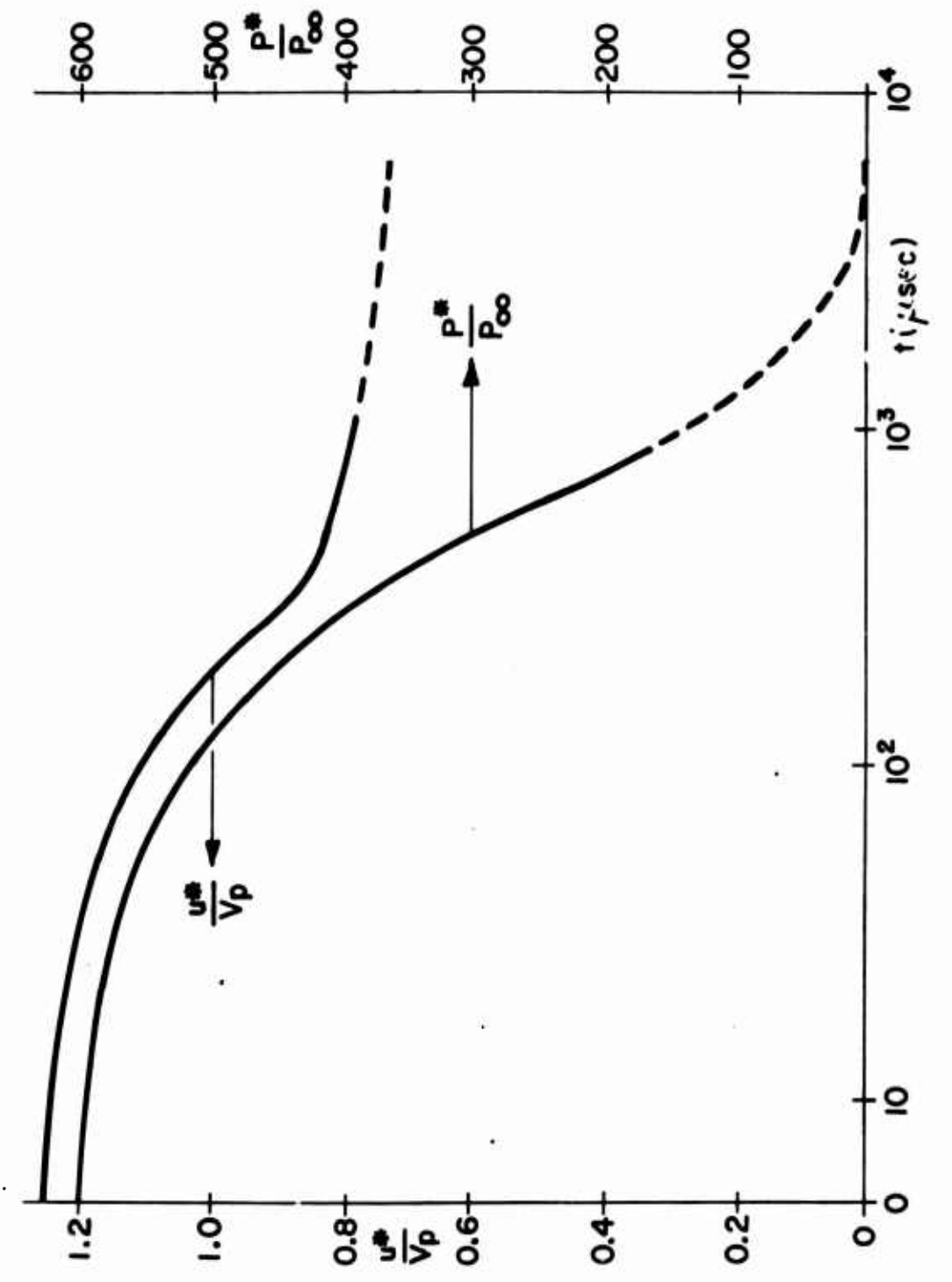

FIGURE 13: M-16 Muzzle Exit Conditions

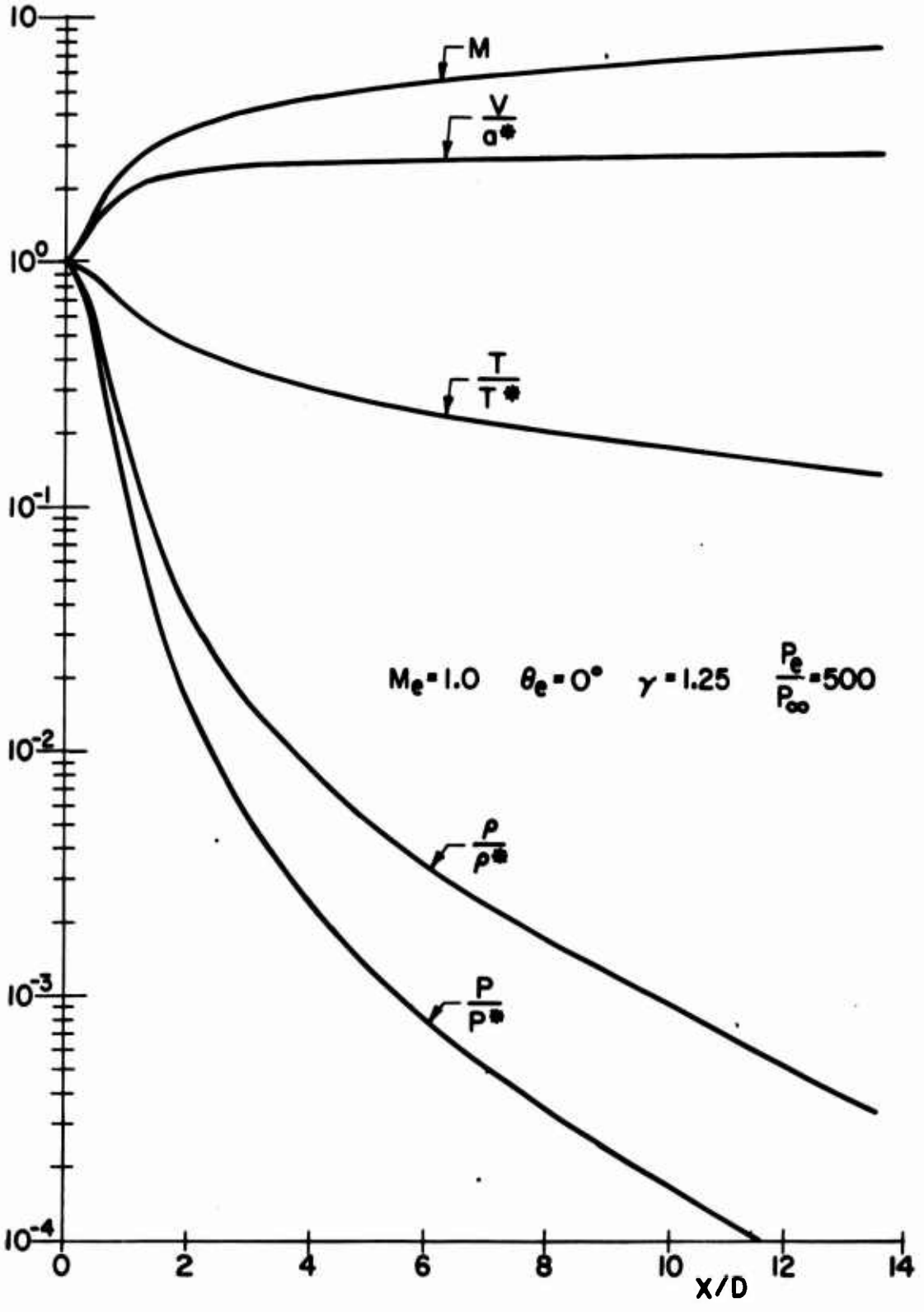

FIGURE 14: Property Distribution Along Jet Centerline

(A) x/D = 0.8

(B) x/D = 1.2

FIGURE 15: Bare Muzzle

FIGURE 16: Deflector Mounted, x/D = 2.0

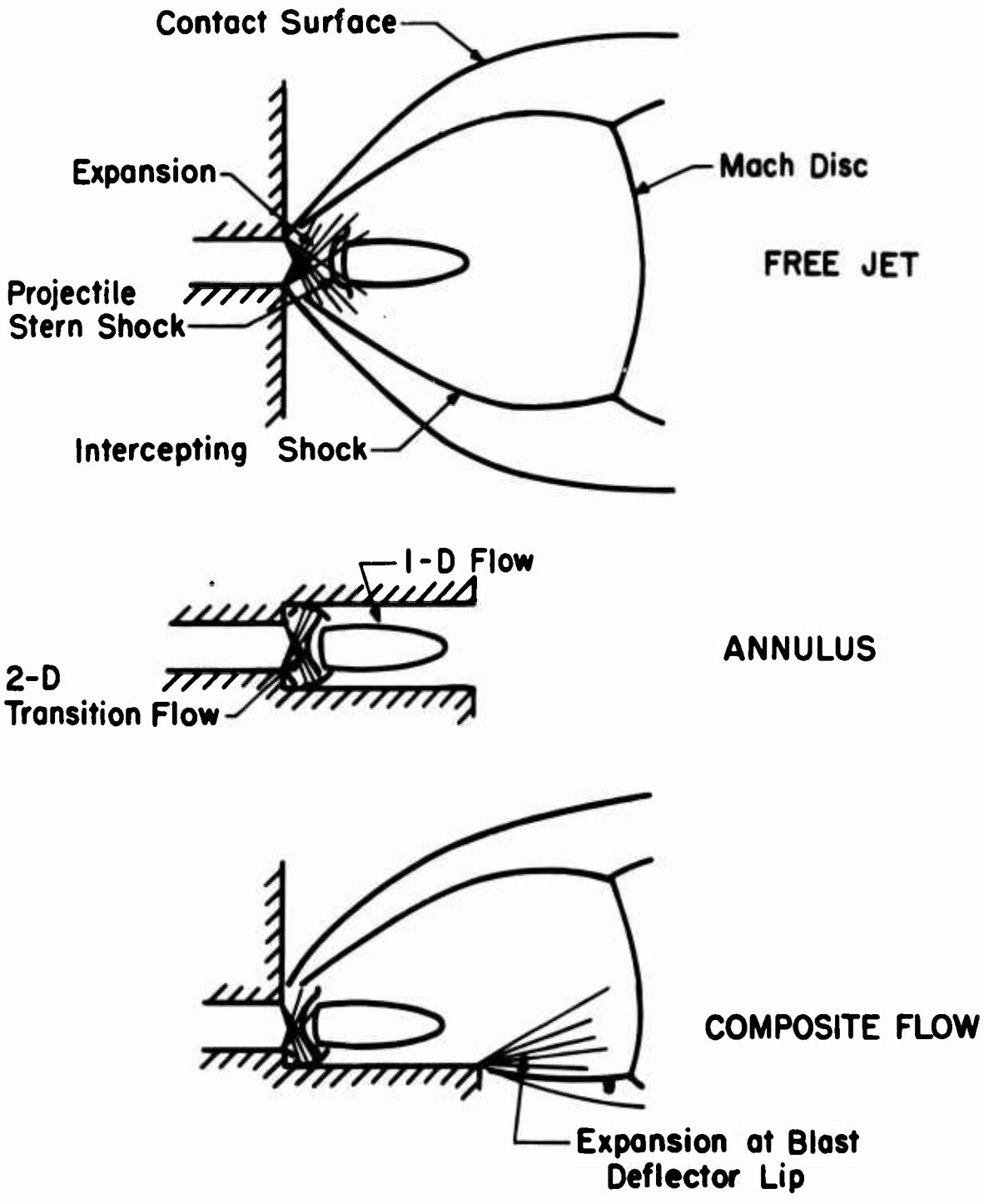

FIGURE 17: Steady Flow Models

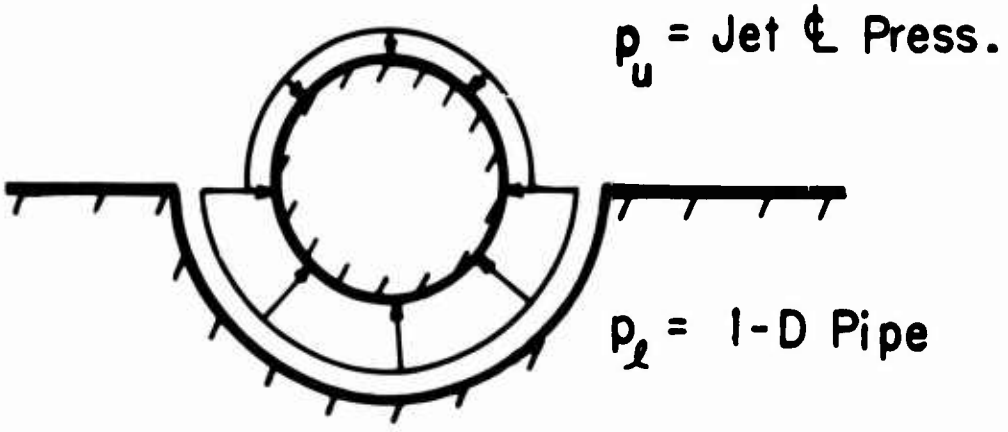

FIGURE 18: Pressure Discontinuity in Plate Plane

FIGURE 19: 1-D Unsteady Analog of Expansion

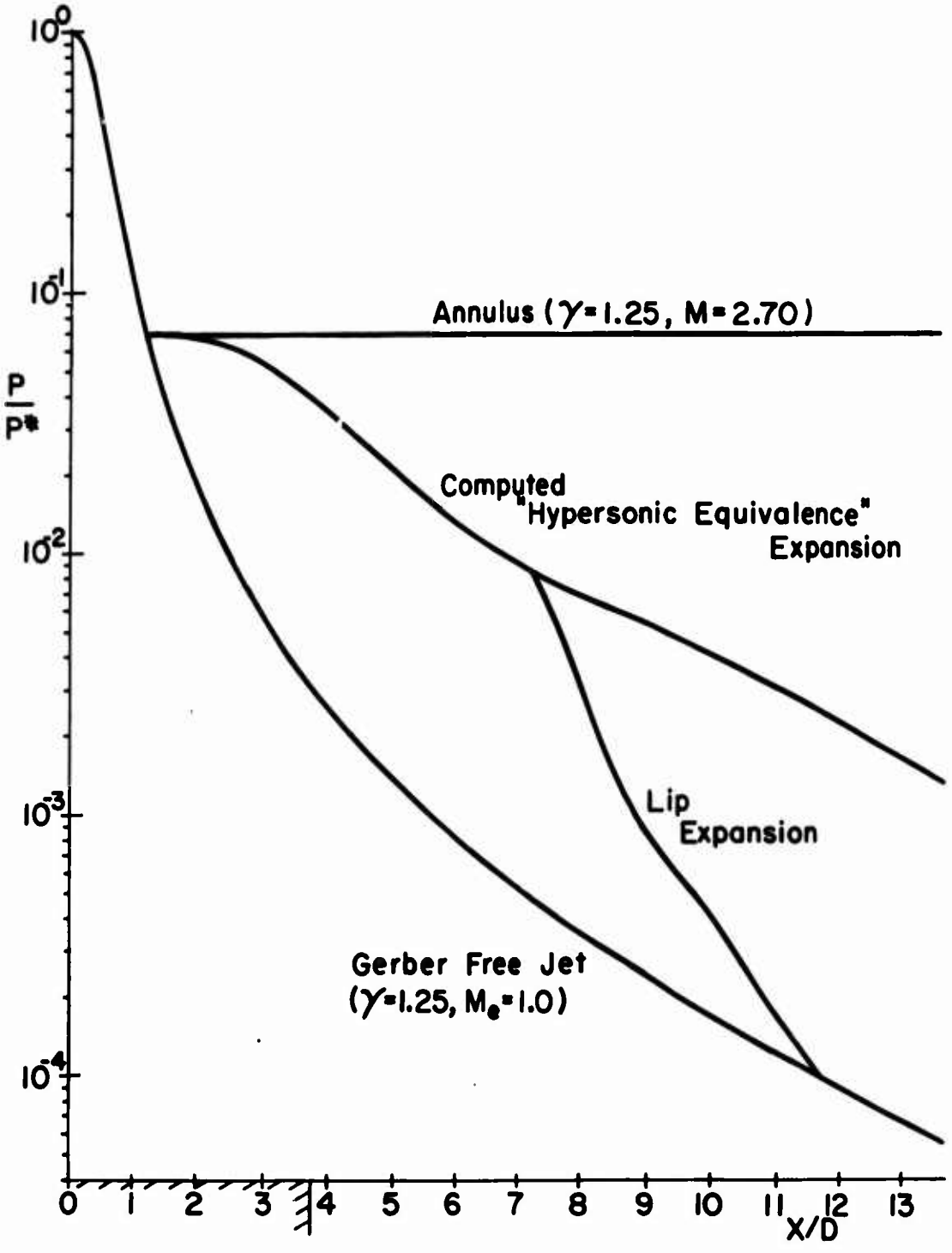

FIGURE 20: Longitudinal Pressure Distributions

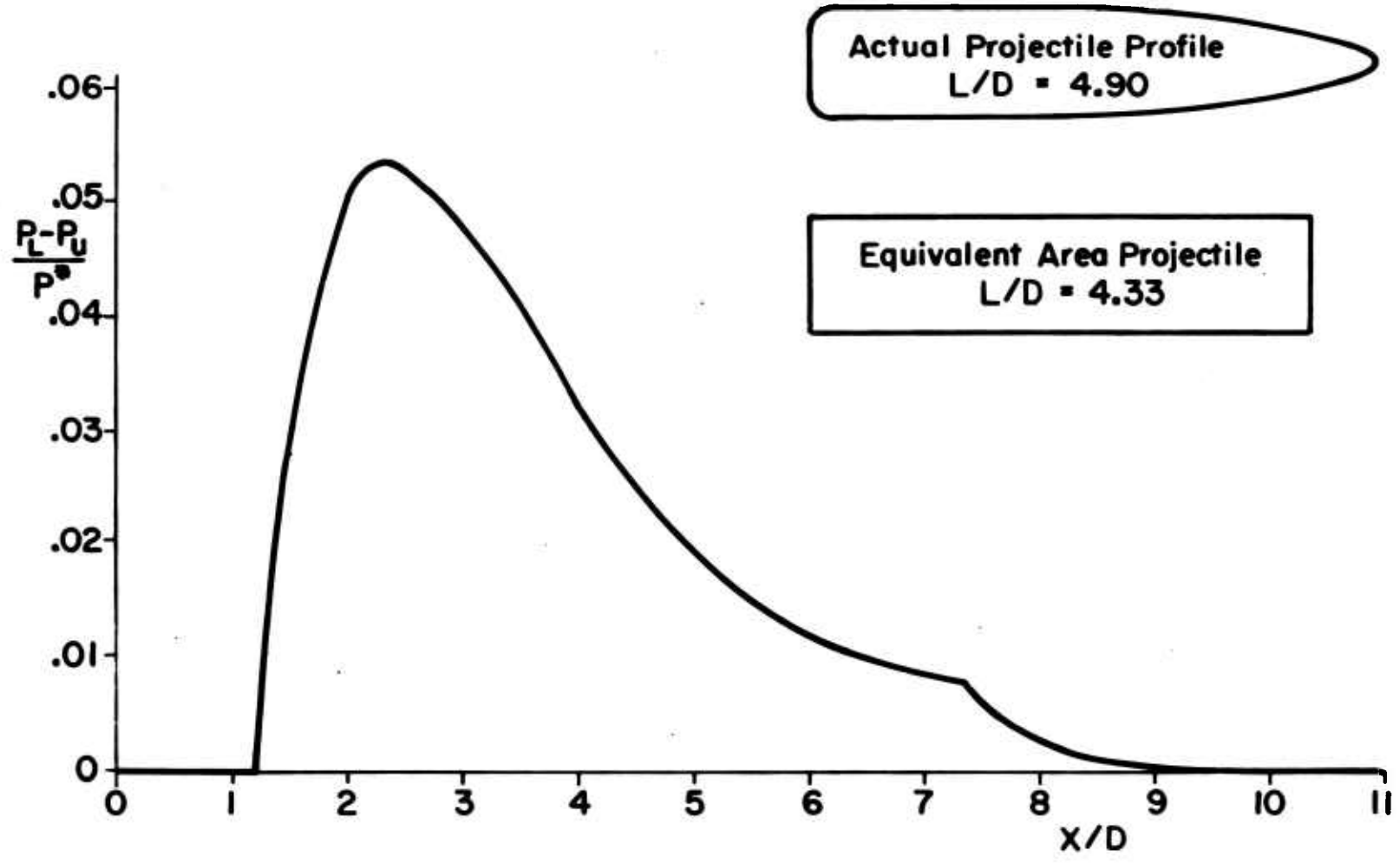

FIGURE 21: Mean Pressure Differential Across Projectile

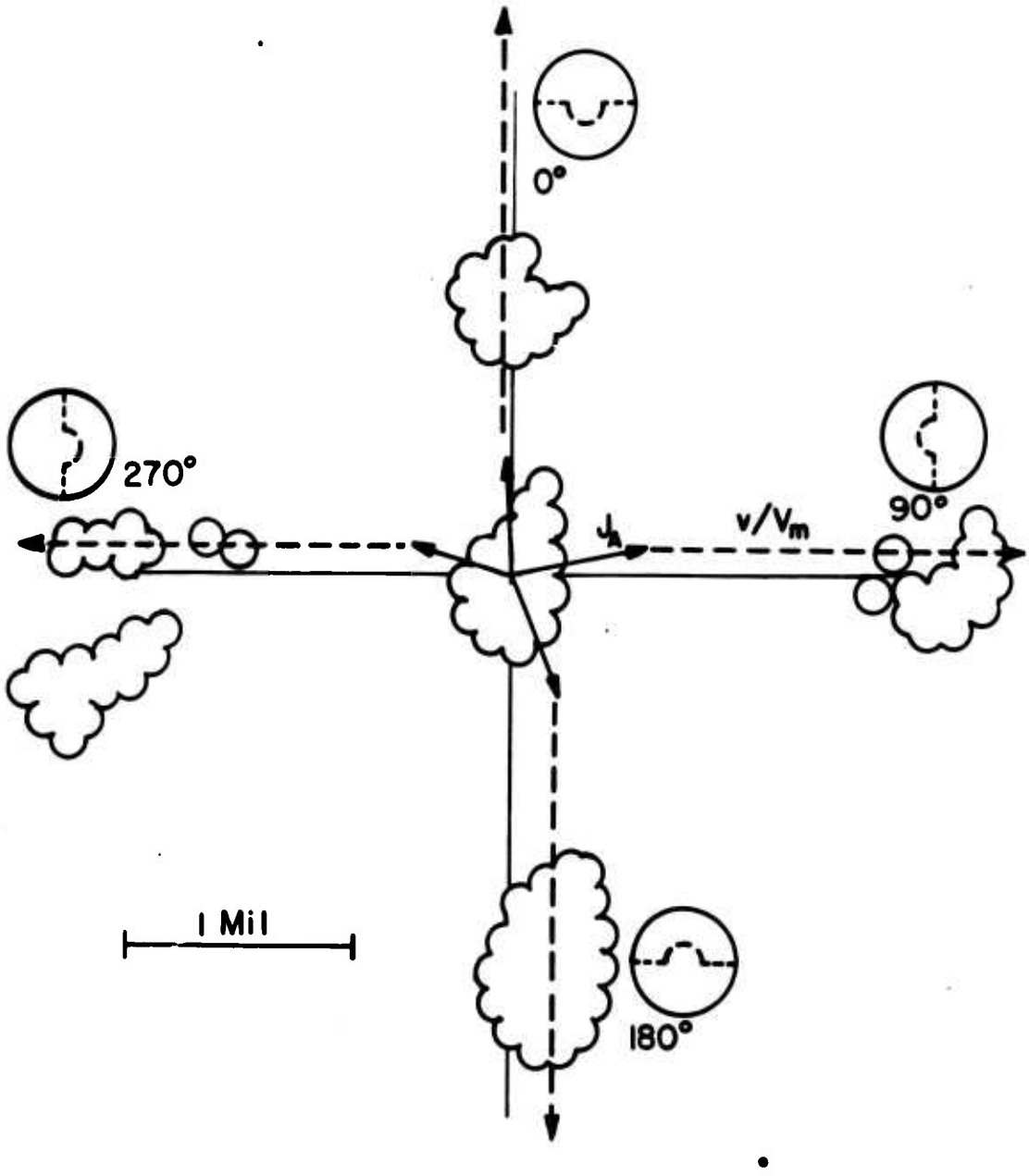

FIGURE 22: Yaw Card Impacts 139 Feet From Muzzle

REFERENCES

1. C. Cranz and B. Glatzel, "Die Ausstromung von Gasen Bei Hohen Anfangsdrucken," Ann. Der Physik, Vol. 43, 1914.

2. P. Quayle, "Spark Photography and its Application to Some Problems in Ballistics," Scientific Papers, Bureau of Standards, Vol. 20, No. 508, 1925.

3. C. Cranz, Lehrbuch Der Ballistik, J. Springer Verlag, Berlin, 1926.

4. K. Oswatitsch, "Intermediate Ballistics," Deutsche Luft und Raumfahrt, FB 64-37, December 1964, AD 473 249.

5. W. Gretler, "Intermediate Ballistics Investigations on Wing Stabilized Projectiles," Deutsche Luft und Raumfahrt, RR 67-92, December 1967.

6. J. I. Erdos and P. D. Del Guidice, "Gas Dynamics of Muzzle Blast," AIAA Paper 74-532, June 1974.

7. J. I. Erdos, P. D. Del Guidice, and M. Visich, "Aerodynamics of Sabot Discard Within a Muzzle Blast Environment," Ballistic Research Laboratories, Contractor Report 149, April 1974.

8. T. D. Taylor, "Calculation of Muzzle Blast Flow Field," Picatinny Arsenal, Report 4155, December 1970, AD 881 523L.

9. F. H. Mallie, "Numerical Calculation of a 105mm Gun Blast with Projectile," Naval Weapons Laboratory, TR 3002, August 1973, AD 770818.

10. F. H. Oertel, "Laser Interferometry of Unsteady, Underexpanded Jets," Ballistic Research Laboratories, Report 1694, January 1974, AD 773664.

11. W. F. Braun, "Aerodynamic Data for Small Arms Projectiles," Ballistic Research Laboratories, Report 1630, January 1973, AD 909757L.

12. W. F. Braun, "The Free Flight Aerodynamics Range," Ballistic Research Laboratories, Report 1048, July 1958, AD 202249.

13. C. H. Murphy, "Free Flight Motion of Symmetric," Ballistic Research Laboratories, Report 1216, July 1963, AD 442757.

14. E. M. Schmidt and D. D. Shear, "The Flow Field About the Muzzle of an M-16 Rifle," Ballistic Research Laboratories, Report 1692, January 1974. (Also, "The Formation and Decay of Impulsive Supersonic Jets," AIAA Paper 74-331, June 1974), AD 916646L.

REFERENCES (Continued)

15. P. Owen and C. Thornhill, "The Flow in an Axially Symmetric Supersonic Jet From a Nearly Sonic Orifice into a Vacuum," Royal Armament Research and Development Establishment, Report 30/48, 1948.

16. A. Barakauskas, "Sudden Expansion of a Bounded Jet at High Pressure Ratio," AIAA Journal, Vol. 2, No. 9, September 1964.

17. R. N. Cox and L. F. Crabtree, Elements of Hypersonic Aerodynamics, Academic Press, New York, 1965.

LIST OF SYMBOLS

C_L	lift coefficient
C_M	moment coefficient
D	projectile diameter
I_a	axial moment of inertia
I_t	transverse moment of inertia
J_A	aerodynamic jump
K	length (radians) or generator of epicycle
L	projectile length
M	Mach number
m	projectile mass
p	pressure
t	time
V_m	muzzle velocity
v	transverse velocity
X	downrange direction
α	angle of attack
β	angle of sideslip
γ	ratio of specific heats
ξ	yaw angle
ϕ	orientation of generator or epicycle

Subscripts

o	at penetration of blast

LIST OF SYMBOLS (Continued)

Superscripts

$( )'$	rate of change of quantity in calibers
$(\dot{})$	time rate of change of quantity
$( )^*$	sonic exit condition

DISTRIBUTION LIST

No. of Copies	Organization
2	Commander Defense Documentation Center ATTN: DDC-TCA Cameron Station Alexandria, Virginia 22314
1	Director Defense Nuclear Agency Washington, DC 20305
1	Commander U.S. Army Materiel Command ATTN: AMCDL 5001 Eisenhower Avenue Alexandria, Virginia 22333
1	Commander U.S. Army Materiel Command ATTN: AMCRD, BG H. A. Griffith 5001 Eisenhower Avenue Alexandria, Virginia 22333
1	Commander U.S. Army Materiel Command ATTN: AMCRD-T 5001 Eisenhower Avenue Alexandria, Virginia 22333
1	Commander U.S. Army Materiel Command ATTN: AMCRD-W 5001 Eisenhower Avenue Alexandria, Virginia 22333
1	Commander U.S. Army Aviation Systems Command ATTN: AMSAV-E 12th and Spruce Streets St. Louis, Missouri 63166
1	Director U.S. Army Air Mobility Research and Development Laboratory Ames Research Center Moffett Field, California 94035
2	Commander U.S. Army Electronics Command ATTN: AMSEL-RD AMSEL-CE Fort Monmouth, New Jersey 07703
2	Commander U.S. Army Missile Command ATTN: AMSMI-R AMSMI-RBL Redstone Arsenal, Alabama 35809
5	Commander U.S. Army Missile Command ATTN: AMSMI-RDK Mr. R. Becht (4 cys) Mr. R. Deep Redstone Arsenal, Alabama 35809
1	Commander U.S. Army Tank Automotive Command ATTN: AMSTA-RHFL Warren, Michigan 48090
2	Commander U.S. Army Mobility Equipment Research & Development Center ATTN: Tech Docu Cen, Bldg. 315 AMSME-RZT Fort Belvoir, Virginia 22060
2	Commander U.S. Army Armament Command ATTN: Technical Library Rodman Laboratories Rock Island, Illinois 61202

DISTRIBUTION LIST

No. of Copies	Organization
6	Commander U.S. Army Frankford Arsenal ATTN: Mr. T. Boldt SARFA-U2100 Mr. J. Mitchell SARFA-U3100, S. Fulton SARFA-U3300 Mr. S. Hirshman Mr. A. Cianciosi L4100-150-2 Mr. C. Sleischer, Jr. Philadelphia, Pennsylvania 19137
8	Commander U.S. Army Picatinny Arsenal ATTN: SARPA-DR-D, S. Wasserman SARPA-DR-V, Mr. A. Loeb Mr. D. Mertz SARPA-D, Mr. Lindner SARPA-V, E. Walbrecht Mr. S. Verner SARPA-VE, Dr. Kaufman Mr. E. Friedman Dover, New Jersey 07801
1	Commander U.S. Army Watervliet Arsenal Watervliet, New York 12189
2	Commander U.S. Army Harry Diamond Laboratories ATTN: AMXDO-TI H. Davis, Branch 420 2800 Powder Mill Road Adelphi, Maryland 20783
1	Commander U.S. Army Materials and Mechanics Research Center ATTN: AMXMR-ATL Watertown, Massachusetts 02172
1	Commander U.S. Army Natick Laboratories ATTN: AMXRE, Dr. D. Sieling Natick, Massachusetts 01762
1	Commander U.S. Army Ballistic Missile Defense Systems Command Huntsville, Alabama 35804
1	Commander U.S. Army Research Office (Durham) ATTN: CRD-AA-EH Box CM, Duke Station Durham, North Carolina 27706
3	Commander U.S. Naval Air Systems Command ATTN: AIR-604 Washington, DC 20360
3	Commander U.S. Naval Ordnance Systems Command ATTN: ORD-9132 Washington, DC 20360
2	Commander and Director U.S. Naval Ship Research and Development Center ATTN: Tech Lib Aerodynamic Lab Washington, DC 20007
3	Commander U.S. Naval Weapons Center ATTN: Code 753, Tech Lib Code 50704, Dr. W. Haseltine Code 3007, Mr. A. Rice China Lake, California 93555

DISTRIBUTION LIST

No. of Copies	Organization
4	Commander U.S. Naval Ordnance Laboratory ATTN: Code 031, Dr. K. Lobb Code 312, Mr. R. Regan Mr. S. Hastings Code 730, Tech Lib Silver Spring, Maryland 20910
3	Director U.S. Naval Research Laboratory ATTN: Tech Info Div Code 7700, D. A. Kolb Code 7720, Dr. E. McClean Washington, DC 20390
3	Commander U.S. Naval Weapons Laboratory ATTN: Code GX, Dr. W. Kemper Mr. F. H. Maille Dr. G. Moore Dahlgren, Virginia 22448
1	Commander U.S. Naval Ordnance Station ATTN: Code FS13A, P. Sewell Indian Head, Maryland 20640
2	ADTC (ADBPS-12) Eglin AFB Florida 32542
1	AFATL (DLR) Eglin AFB Florida 32542
1	AFATL (DLRD) Eglin AFB Florida 32542
1	AFATL (DLRV) Eglin AFB Florida 32542
2	AFATL (DLRA, F. Burgess; Tech Lib) Eglin AFB Florida 32542
1	AFWL (DEV) Kirtland AFB New Mexico 87117
1	ARD (ARIL) Wright-Patterson AFB Ohio 45433
1	ARL Wright-Patterson AFB Ohio 45433
1	ASD (ASBEE) Wright-Patterson AFB Ohio 45433
1	Director National Bureau of Standards ATTN: Tech Lib U.S. Department of Commerce Washington, DC 20234
1	Headquarters National Aeronautics and Space Administration ATTN: Code EP, M. Adams Washington, DC 20546
1	Director NASA Scientific and Technical Information Facility ATTN: SAK/DL P.O. Box 33 College Park, Maryland 20740
1	Director Jet Propulsion Laboratory ATTN: Tech Lib 4800 Oak Grove Drive Pasadena, California 91103

DISTRIBUTION LIST

No. of Copies	Organization
2	Director National Aeronautics and Space Administration George C. Marshall Space Flight Center ATTN: MS-I, Lib R-AERO-AE, Mr. A. Felix Huntsville, Alabama 35812
1	Director National Aeronautics and Space Administration Langley Research Center ATTN: MS 185, Tech Lib Langley Station Hampton, Virginia 23365
1	Director National Aeronautics and Space Administration Lewis Research Center ATTN: MS 60-3, Tech Lib 2100 Brookpark Road Cleveland, Ohio 44135
1	Advanced Technology Laboratories ATTN: Dr. J. Erdos Merrick & Stewart Avenues Westbury, New York 11590
2	ARO, Inc. ATTN: Tech Lib Arnold AFS Tennessee 37389
1	Calspan Corporation ATTN: Mr. G. A. Sterbutzel P.O. Box 235 Buffalo, New York 14221
1	Technical Director Colt Firearms Corporation 150 Huyshore Avenue Hartford, Connecticut 14061
1	General Electric Corporation Armaments Division ATTN: Mr. R. Whyte Lakeside Avenue Burlington, Vermont 05401
1	Winchester-Western Division Olin Corporation ATTN: Mr. D. Merrill New Haven, Connecticut 06504
1	Sandia Laboratories ATTN: Aerodynamics Dept Org 9320, R. Maydew P.O. Box 5800 Albuquerque, New Mexico 87115
1	Guggenheim Aeronautical Laboratory California Institute of Technology ATTN: Tech Lib Pasadena, California 91104
2	Franklin Institute ATTN: Dr. Carfagno Dr. Wachtell Race & 20th Streets Philadelphia, Pennsylvania 19103
1	Director Applied Physics Laboratory The Johns Hopkins University 8621 Georgia Avenue Silver Spring, Maryland 20910
1	Massachusetts Institute of Technology Department of Aeronautics and Astronautics ATTN: Tech Lib 77 Massachusetts Avenue Cambridge, Massachusetts 02139

DISTRIBUTION LIST

No. of Copies	Organization
1	Ohio State University Department of Aeronautics and Astronautical Engineering ATTN: Tech Lib Columbus, Ohio 43210
2	Polytechnic Institute of Brooklyn Graduate Center ATTN: Dr. G. Morretti Dr. R. Cresci Farmingdale, New York 11735
1	Director Forrestal Research Center Princeton University Princeton, New Jersey 08540
1	Princeton University Forrestal Laboratories ATTN: Dr. S. I. Cheng Princeton, New Jersey 08540
1	Southwest Research Institute ATTN: Mr. Peter S. Westine P.O. Drawer 28510 8500 Culebra Road San Antonio, Texas 78228
2	University of Michigan Department of Aeronautical Engineering ATTN: Dr. A. Kuethe Dr. M. Sichel East Engineering Building Ann Arbor, Michigan 48104
1	Northrop Corporation Aircraft Division ATTN: Dr. A. Wortman 3901 W. Broadway Hawthorne, California 90250
	Aberdeen Proving Ground
	Marine Corps Ln Ofc Cdr, USATECOM ATTN: AMSTE-BE Mr. Morrow AMSTE-TA-R Mr. Wise Dir, USAMSAA